UNIVERSITY OF CALIFORNIA,
IRVINE

Advances in RNA Optogenetic Tools

DISSERTATION

submitted in partial satisfaction of the requirements
for the degree of

DOCTOR OF PHILOSOPHY

in Pharmacological Sciences

by

Kelly Alexis Rotstan

Dissertation Committee:
Professor Andrej Lupták, Chair
Professor Richard Chamberlin
Professor Klemens J. Hertel

2019

DEDICATION

To

my husband, David
my parents, Robert and Ilene, and my brother, Sean
for their endless support and love.

TABLE OF CONTENTS

LIST OF FIGURES

LIST OF TABLES

ACKNOWLEDGMENTS

I would like to express the deepest appreciation to my advisor and committee chair, Professor Andrej Lupták, for his immense support, patience, motivation, enthusiasm and knowledge. I would not have made it this far without your guidance and willingness to conquer challenging obstacles together, in science and with my health. It is rare to find a mentor who embodies so many wonderful traits. Thank you for shaping me into a great scientist and for making my PhD a memorable experience. It would be impossible to count all of the ways you have helped me in my career. Thank you.

My sincere appreciation also goes to my committee members, Professor A. Richard Chamberlin and Professor Klemens J. Hertel, for their insightful comments, encouragement, and valuable advice. Professor Chamberlin, thank you for always believing in me. I would not have finished my PhD without your extensive help and expertise.

My dissertation work received funding from the National Science Foundation and the National Institutes of Health. A special thank you to the Chemistry and Structural Biology fellowship at UC Irvine (through NIH) for financially supporting me for two years.

My doctor, Daniel Wallace, also deserves special recognition for making this achievement possible. To all of those fighting an illness, this PhD is for you.

I also thank all current and past members of the Lupták lab for their unending support throughout my time at UC Irvine. Your friendship and endless coffee trips made this journey more enjoyable!

I'd like to acknowledge my wonderful friends who have also supported me on this difficult journey. There are too many of you to list, but you know who you are! Thank you for making my life so fun and beautiful!

Thank you to my wonderful family for their constant love and support. Mom and Dad, thank you for believing in me and for supporting me through all of the ups and downs of my PhD journey. I am so grateful to have you as my parents! Let's celebrate!

Lastly, I'd like to thank my amazing husband, David, for his unfailing love, patience, and wisdom. This accomplishment would not have been possible without your encouragement, advice, and support. Thank you for being my rock in all of the hardships and celebrations during my PhD and life. You are the greatest blessing in my life and there are no words to express my love and gratitude for you. I am beyond thankful that I went to that NSF grant writing session (thank you Lori Greene) – it made this entire experience worth it! I love you hubby!!!

Kelly A. Rotstan

Passionate, detail-oriented scientist with 6+ years of experience working on research projects involving structural biology and biochemistry.

EDUCATION

University of California, Irvine
Irvine, CA
Doctor of Philosophy in Pharmacological Science
Nov. 2019
GPA: 3.92/4.00

Fellowships:
NIH Chemical and Structural Biology Fellow (2017 – 2019)

University of Puget Sound
Tacoma, WA
Bachelor of Science in Biology
Aug. 2014
Minor in Mathematics
GPA: 3.36/4.00

RESEARCH EXPERIENCE

University of California, Irvine: Department of Pharmaceutical Science
Irvine, CA
Advisor: Andrej Luptak *Dec. 2016 – Present*
Discovered and characterized a novel photo-induced riboswitch, Werewolf-1, for application in optogenetic RNA tools. Designed and cloned bacterial and eukaryotic systems for analysis. Performed spectroscopy, fluorometry, luciferase assays, HPLC, and NMR. Analyzed fundamental properties of potential photoriboswitches from an *in vitro* selected pool. Co-wrote an NSF grant (funded) and NIH RO1 grant (unfunded). First author on an *eLife* manuscript.

University of California, Irvine: Department of Pharmaceutical Science
Irvine, CA
Advisor: Mahtab Jafari *Apr. 2016 – Dec. 2016*
Tested the molecular active components from *Rhodiola rosea* on melanoma cell lines, primary keratinocytes, primary fibroblasts, and primary melanocytes. Performed cell proliferation assays and growth assays to assess the toxicity of the active compounds. Assessed whether the putative active molecules protected cell lines from DNA damage caused by UVA/UVB exposure. Learned fly maintenance techniques and studied the impact of *R. rosea* on the fly microbiome via DNA extraction and PCR.

University of California, Irvine: Department of Pharmaceutical Science
Irvine, CA
Advisor: Claudia Benavente – Winter Rotation *Jan. 2016 – Mar. 2016*
Transfected human mesenchymal stem cells and 293T cells to overexpress UHRF1, an epigenetic regulator thought to play a role in pediatric osteosarcoma. Completed lentiviral

transfections, calcium chloride transformations, and electroporation to obtain the desired results. Analysed protein expression via western blotting.

University of California, Irvine: Department of Pharmaceutical Science
Irvine, CA
Advisor: Weian Zhao – Summer Rotation *Jun. 2015 – Oct. 2015*
Engineered stem cells and extracellular vesicles (exosomes) to target cancer. Differentiated cells in different lineages – osteoblasts, adipocytes, and chondrocytes (from human mesenchymal stem cells), macrophages, osteoclasts, and dendritic cells (from murine bone marrow isolation). Learned laboratory techniques including plasmid amplification and analysis, protein quantification, flow cytometry assays, bone-marrow isolation, and mice handling and breeding.

University of Puget Sound: Department of Biology
Tacoma, WA
Advisor: Andreas Madlung *Aug. 2012 – Jan. 2015*
Assessed phototropic and gravitropic response in *lazy*-2 mutant tomato plants. Generated double mutants, containing an auxin-reporter gene, via genetic crossing. Performed transcriptional analysis using GUS staining. Studied growth kinetics using time-lapse and computational analysis. Identified that the *lz-2* mutation leads to a reversal in the gravity response because of a reversal in the direction of auxin transport.

TEACHING EXPERIENCE

University of California, Irvine: Department of Pharmaceutical Sciences
Irvine, CA
Teaching Assistant, Medicinal Chemistry *Jan. 2017 – Jun. 2017*
Teach undergraduates laboratory techniques and protocols, including *in* vitro selection, high throughput screening, and computational docking. Instruct and assist students by holding office hours and leading discussion sections. Provide thorough feedback to students by way of grading lab reports and lab quizzes. Demonstrate the ability to uphold effective student–teacher relationships and impart information through excellent instructional and written communication skills.

University of California, Irvine: Department of Pharmaceutical Sciences
Irvine, CA
Teaching Assistant, *Life 101* *Aug. 2016 – Sep. 2016*
Helped students understand the impact of nutrition, exercise, and lifestyle choices on mental and physical health by providing impactful feedback to assist and instruct students throughout the course. Monitored student interactions and discussions online. Accommodated students by offering additional online instruction and support via email.

University of California, Irvine: Department of Pharmaceutical Sciences
Irvine, CA
Teaching Assistant, *Molecular Pharmacology II* *Mar. 2016 – Jun. 2016*
Offered dynamic instruction to assist students in successfully completing and understanding coursework. Taught two discussion sections per week and created

worksheets that reviewed course material. Held office hours to individually help students with questions.

Future Focused
San Juan Capistrano, CA
Tutor *Mar. 2015 – Sep. 2015*
Provided individual assistance to high school students in a broad range of chemistry, math, and biology courses. Helped students improve study habits and overall course performance by reviewing course material, practicing problems, and answering students' questions.

MENTORING & OUTREACH

LEAP Into Science, National Science Foundation – Luptak Laboratories
Irvine, CA *Dec. 2016 – Present*
Instruct middle school students on DNA extraction from strawberries and how to run and analyze "murder mystery" DNA samples on an agarose gel. Effectively communicate and demonstrate science as well as encourage younger audiences to pursue further studies in STEM disciplines.

Science Saturdays at UCI – Luptak Laboratories
Irvine, CA *Dec. 2016 – Present*
Assist middle school students in conducting their own small experiment in the Luptak laboratories. Instruct and guide students efficiently. Encourage students to continue their education in science.

Student Mentor – Jafari Laboratory
Irvine, CA *Apr. 2016 – Dec. 2016*
Advised six undergraduate students on conducting research in the Jafari Laboratory. Created and planned independent projects for each student, and taught students the necessary tools for completing their project. Supervised laboratory work, discussed research results, and offered guidance for successful completion of laboratory experiments. Took students to their first science conference.

Mentor and Tutor – Jason Lee Middle School
Tacoma, WA Jul. *2014 – Dec. 2014*
Taught English, science, and math to low-income students at Jason Lee Middle School. Supervised various activities in the afterschool program, including physical education, crafts, tutoring, etc. Encouraged students to pursue their education and life goals.

Student Tutor – Phi Sigma Biological Sciences Honor Society, University of Puget Sound
Tacoma, WA Aug. *2013 – May 2014*
Tutored biology and chemistry students from the University of Puget Sound (UPS) once a week. Held office hours to inform UPS students about research opportunities at our university.

First Book – McArver Elementary School
Tacoma, WA *Mar. 2011 – May 2014*
Provided free books to children from low-income families at McArver Elementary School. Read books to children and tutored them in basic subjects.

Champions are Readers – Tacoma Rescue Mission
Tacoma, WA *Mar. 2011 – May 2014*
Helped underprivileged kindergarten and elementary students read and develop reading strategies. Incorporated crafts and projects into our reading sessions to encourage students to read.

PUBLICATIONS

Rotstan, K. A. *et al.* Regulation of mRNA translation by a photoriboswitch. *eLife.* (2019), *under review*.

Senior Thesis: **Rotstan, K. A.** Assessing the phototropic and gravitropic response in *lazy* 2 mutants. (2014).

PRESENTATIONS

Synthetic and Chemical Biology Seminar (oral) *Feb. 2018*

Phi Sigma Research Symposium (oral) *Apr. 2014*

Washington NASA Space Grant Conference (poster) *Aug. 2013*

Phi Sigma Research Symposium (poster) *Jun. 2013*

Phi Sigma Research Symposium (oral) *Apr.2013*

AWARDS

NIH - CSB Trainee (5T32GM108561-04)
Summer, 2017 - 2019
NSF GRFP Honorable Mention
Spring, 2016
Dean's List
Spring, 2014
Pi Beta Phi Academic Scholar
Spring, 2014
University of Puget Sound Enrichment Committee (UEC) Student Research Award
Spring, 2014
UEC Student Research Award
Fall, 2013
Dean's List
Fall, 2013
NASA Space Grant Summer Undergraduate Researcher
Summer, 2013

University of Puget Sound Summer Research Scholar
Summer, 2013
UEC Student Research Award
Summer, 2013
UEC Student Research Award
Spring, 2013
UEC Student Research Award
Fall, 2012
UEC Student Research Award
Summer, 2012
Puget Sound Trustee Scholarship
2010 - 2014

AFFILIATIONS

Phi Sigma Biological Sciences Honor Society member (2013 – Present), NASA Space Grant Scholar (2013)

ABSTRACT OF THE DISSERTATION

Advances in RNA Optogenetic Tools
By

Kelly Alexis Rotstan

Doctor of Philosophy in Pharmacological Sciences

University of California, Irvine, 2019

Professor Andrej Lupták, Chair

There is a need to develop and expand approaches to regulate and alter the function of RNA using light. Although there are many optogenetic tools involving light-responsive proteins, RNA tools remain underdeveloped. The highly useful nature of RNA makes them valuable tools in regulating intracellular functions. For example, riboswitches are RNAs that mediate gene expression in archaea, plants, and fungi and play significant roles in feedback mechanisms. Other RNAs, like ribozymes, have enzymatic activity and can self-cleave in the presence of adequate concentrations of its metabolite. The functionality of RNA has grasped the attention of synthetic biologists in recent years, leading to new discoveries and the start of RNA optogenetic tools.

In this thesis, I report the first example of a riboswitch that can reversibly regulate translation in response to a sub-millisecond pulse of light *in vivo*. This is the first optogenetic tool that is a light-regulated RNA switch that responds to a reversible photoactive ligand to control gene expression, giving great spatial and temporal resolution. This work also investigates two more potential photoriboswitches, significantly expanding the field of optogenetic RNA tools.

Chapter 1: Introduction

1.1 Background

Light is perhaps the most widely employed tool to interrogate biological specimens. Starting first with optical microscopes through present-day super-resolution and optogenetic probes, visible light has provided a vast amount of information about the state of living systems[1]. Light-actuated tools are advantageous for their exceptional spatiotemporal precision and sensitivity, allowing for fast and reversible control of target sites[2]. The wavelength and intensity of incident light can also be precisely tuned and measured, enabling applications in quantitative optogenetic regulation and single molecule detection[3,4].

Synthetic biology has made remarkable progress in our ability to control gene expression with light. Optogenetic techniques have transformed the sciences by using photoreceptors to control biological events in an extremely fast and precise manner. Natural photoreceptors have been employed in the design of optogenetic tools, in which the use of opsins helped transform the neuroscience field by activating and silencing specific cells with great precision[5,6]. Additionally, photoreceptors have been used as templates for engineering fluorescent proteins, including light-oxygen-voltage-sensing (LOV)-based fluorescent proteins that have been used as reporters in bacteria and mammalian cells[7,8].

Light has been linked to proteins for many years and remains the repertoire of optogenetic molecular tools available to scientists; however, the same kind of molecular tools can be applied to the field of RNA biology. Contrasting the central dogma of molecular biology, which states that RNA only acts as an intermediary messenger

between DNA and proteins, RNA molecules actively participate in catalyzing and regulating many cellular processes—roles that were previously assigned to only proteins[9–13]. Riboswitches, for example, are small regulatory RNAs that can fold and selectively bind a specific metabolite within seconds of their synthesis [14,15]. Upon ligand binding, riboswitches undergo a conformational change that mediates gene expression [16,17]. Because riboswitches act fast, they can be used to regulate many co-transcriptional events: from folding of self-splicing ribozymes and protein binding of regulatory domains of mRNA untranslated regions to the assembly of splicing-related complexes (including those that regulate alternative splicing). Riboswitches can also regulate slower co-transcriptional events that depend on structured RNAs, such as gene expression regulation by non-coding RNAs [18]. Riboswitches' unique function can be used to develop new molecular biology tools, including utilizing light to control gene expression.

In summary, as research progresses, the functionality of RNA seems to increase and thus there is a need for new RNA optogenetic tools in order to interrogate RNA *in vivo* and to optically activate and trace single RNAs in live tissues. My thesis work focuses on new RNA optogenetic tools, specifically a novel photoriboswitch that can regulate gene expression with a pulse of light. An overview of riboswitches and the current RNA optogenetic tools are briefly described below.

1.2 Riboswitches

Since their discovery in 2002, approximately 40 classes of riboswitches have been identified in various bacterial species to date and it is proposed that thousands of

riboswitches remain to be found within the DNA of bacteria [19–21]. In nature, riboswitches are commonly found in the 5' untranslated regions (UTRs) of mRNAs where they often respond to cellular metabolites, playing a crucial role in feedback regulatory mechanisms [16,17,22,23]. Riboswitches consist of two main domains: an aptamer domain, where molecular recognition and ligand-binding takes place, and an expression platform, where regulation of gene expression occurs. Feedback mechanisms occur when the metabolite abundance exceeds its threshold and binds to the riboswitch's aptamer domain, initiating a conformational change in the expression platform and thereby regulating gene expression[24].

There are two main types of riboswitches—those that regulate transcription via the formation of a *rho*-independent terminator to turn transcription 'OFF' and an antiterminator hairpin to turn transcription 'ON', and those that regulate translation via the formation of a hairpin that sequesters the ribosomal binding site (RBS) and partially-complementary helix that exposes the RBS (Figure 1.1). The primary mechanism of action by riboswitches is transcriptional termination, a regulatory mechanism used to halt mRNA synthesis to save bacteria energy from producing unnecessary full-length mRNAs [25].

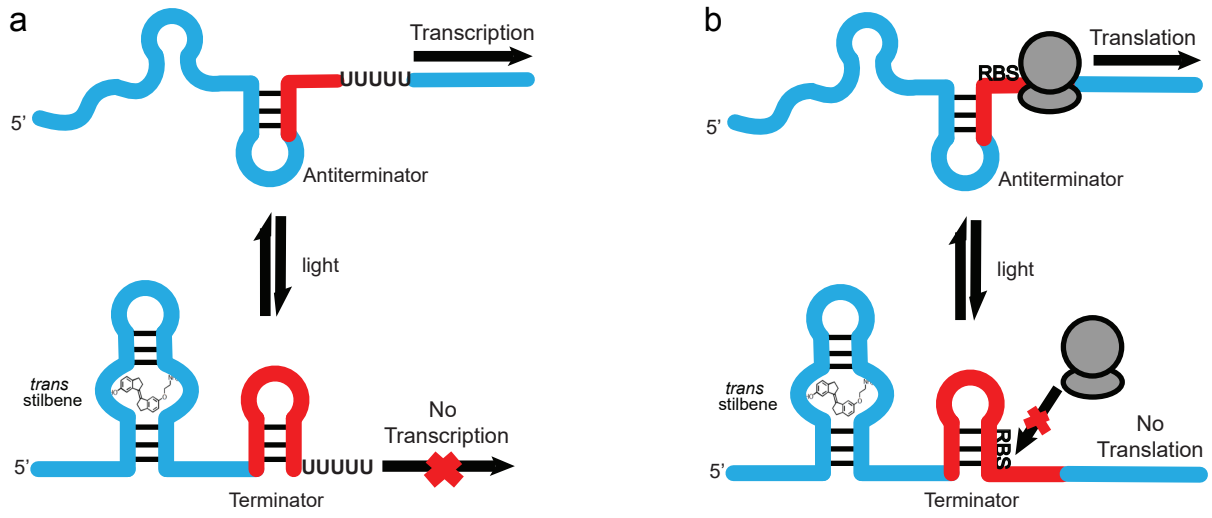

Figure 1.1 Schematic of transcription and translation by a riboswitch. a, Regulation of transcription by a riboswitch. When no ligand is present, an antiterminator helix is formed, allowing for transcription to occur. In the presence of ligand, the riboswitch binds the ligand, leading to the formation of a terminator hairpin that terminates transcription. **b,** Regulation of translation by a riboswitch. When no ligand is present, the ribosomal binding site is accessible for translation to occur. When ligand is present, it binds the aptamer domain thereby forming a terminator hairpin that sequesters the ribosomal binding site, shutting down translation.

Riboswitches have become significant in synthetic biology due to their natural ability to regulate gene expression. The potential of riboswitches to be engineered into artificial genetic control devices in biotechnology makes them valuable tools in the RNA world. Riboswitches have the ability to respond to any ligand of choice, act on both a transcriptional and post-transcriptional level, and are versatile and robust[26,27]. For

example, the addition of an inhibitory stem-loop close to the ribosomal binding site (RBS) was used to construct a riboswitch based on helix slippage in bacteria[28,29].

1.3 Light-Up RNA Aptamers

The field of optogenetics first focused on RNA being a carrier of visual information, directing the RNA field to discover an array of light-up aptamers. Historically, RNA was first detected using specific probes, such as antibodies or oligonucleotides, that were fluorescently labelled[30]. The need for better detection in order to reach single-molecule sensitivity paved the way for the discovery of RNAs that specifically interact and bind a fluorogen to form a fluorescent complex, termed fluorogenic aptamers, or light-up aptamers[31] (Figure 1.2).

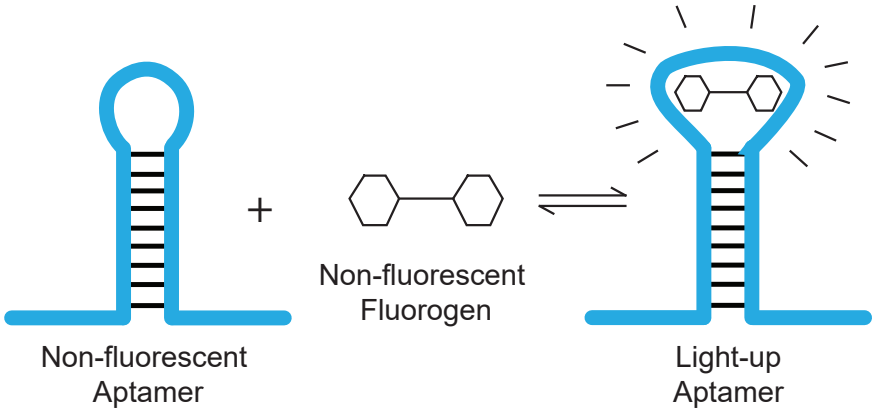

Figure 1.2 Illustration of a fluorogenic aptamer. Fluorogenic aptamers, or light-up aptamers, are aptamers that bind a non-fluorescent fluorogen to form a fluorescent complex.

Spinach, Broccoli, and Mango are some of the most iconic light-up aptamers, and each were generated from an RNA pool using systematic evolution of ligands by exponential enrichment (SELEX) to enrich for their unique sequence[32–36]. These aptamers helped advance the RNA field, enabling the visualization of RNA molecules within a cell with higher contrast compared to previous systems used to detect RNA, like fluorescence *in situ* hybridization[37]. Over the past decade, many fluorogenic aptamers have been discovered, covering the entire visible spectrum, and contributing to the development of high-throughput drug screening pipelines [31]. Additionally, fluorogenic aptamers have been used as tools for designing new RNA aptamer-biosensors that fused the fluorophore–aptamer domain to new RNAs to trace metabolite-bound sensors and RNA processes in cells[38–42]. This contributed to transforming RNA optogenetics from focusing on visual information into being coupled with tools that use light to influence a diverse range of key molecular events, from gene expression to neuron spiking[43–46]. However, there is still a need to develop new optogenetic tools because detection of these fluorogenic aptamers is still masked by some autofluorescence, yielding background signal that prevents single-molecule sensitivity[38–40,47–50].

1.4 Optogenetic Molecular Tools to Study RNA Gene Regulation

Ribozyme switches, or aptazymes, can be cloned into multiple points of gene expression pathways, enabling RNA regulation at different stages, such as transcription, splicing, mRNA stability, and translation[51] (Figure 1.3). Previous studies have used light

to control splicing by utilizing photocleavable-backbone linkers on synthetic oligonucleotides in mammalian cells[52,53], however, photocleavage is irreversible, providing only an "ON/OFF" approach. Variants of photo-caged guanines, which can be uncaged with UV light, have also been used to regulate mRNA[54,55] but this process indirectly controls RNA and their photo-uncaging procedures require extensive UV light exposure and are also irreversible, allowing only a single molecular event to be initiated[52,55–58]. Additionally, these processes are often too slow to act co-transcriptionally to affect events like RNA folding, splicing, and processing.

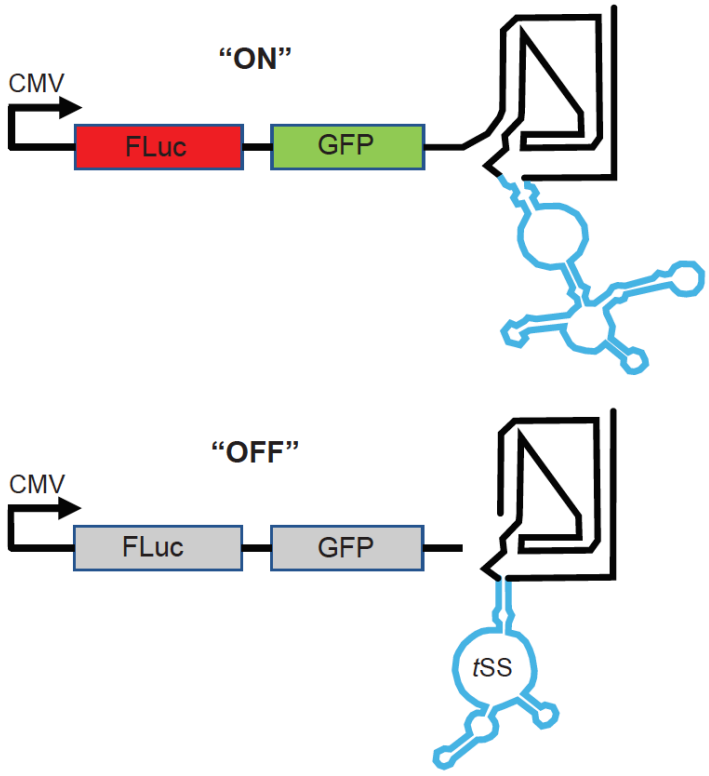

Figure 1.3 Schematic of an engineered aptazyme. An aptazyme is incorporated into the 3' UTR of a dual reporter Firefly luciferase – green fluorescent protein (FLuc – GFP) plasmid. In absence of ligand, the aptazyme is unstable and does not cleave, producing

fluorescent signal. In the presence of ligand (tSS), the aptazyme is stable, and self-cleaving occurs.

Additionally, a previous study discovered a light-responsive aptamer for an azobenzene derivative that binds only one isoform of the ligand, allowing for photocontrol of the RNA *in vitro*[59]. The authors successfully show multiple switching cycles of the ligand binding to the aptamer and being sequestered after light exposure, suggesting that this aptamer could be useful as an optogenetic tool if it was engineered to a riboswitch expression platform or ribozyme loop. However, the authors were unsuccessful at obtaining a riboswitch that binds their ligand and only obtained binding data *in vitro*.

Recently, a bacterial LOV photoreceptor sequence, PAL, was identified to specifically bind a short RNA stem loop with 20 nM affinity in blue light and weaker than 1 μM in darkness[60]. The PAL-RNA interaction is light activated, regulating gene expression at the RNA level in both bacteria and mammalian cells. This study shows the first reversible RNA regulation in mammalian cells; however, the regulation of the system is slow, resulting in one-minute light exposure for activation and ten minutes darkness for inactivation. Thus, a need for more reversible tools with better spatiotemporal precision are needed to regulate RNA *in vivo*.

While there are tools available to trigger signal transduction pathways via light-sensing receptors, there are currently no photoreversible molecules that can reversibly regulate gene expression at the RNA level. Because a light-induced conformational

switch is of key interest, photoreversible molecules, such as stilbenes, are optimal targets for RNA selections.

Photoreversible probes are valuable tools for studying the regulation of complex systems due to their spatiotemporal precision and ability to quickly manipulate events[61,62]. From naturally-occurring photoswitches, like channelrhodopsins that isomerize *trans* retinal to the *cis* isoform, to synthetic azobenzenes that adopt Z and E configurations upon excitation with UV light, photoactive ligands have diversely contributed to the field of optogenetics and our understanding of biological systems[43,63]. The ability to control the activity of biomolecules in a reversible manner has outstanding potential to expand our knowledge on the complex RNA processes that occur in living cells[64,65]. The work in this thesis expands the available RNA toolset by providing the first reversible light-controlled RNA switch that regulates translation *in vitro* and *in vivo*.

1.5 References

1. Chen, X., Zheng, B. & Liu, H. Optical and digital microscopic imaging techniques and applications in pathology. *Anal. Cell. Pathol. (Amst).* **34,** 5–18 (2011).
2. Liu, Q. & Tucker, C. L. Engineering genetically-encoded tools for optogenetic control of protein activity. *Curr. Opin. Chem. Biol.* **40,** 17–23 (2017).
3. Pathak, G. P., Vrana, J. D. & Tucker, C. L. Optogenetic control of cell function using engineered photoreceptors. *Biol. Cell* **105,** 59–72 (2013).
4. Choudhury, S. R. *et al.* Optogenetic regulation of site-specific subtelomeric DNA methylation. *Oncotarget* **7,** 50380–50391 (2016).
5. Shcherbakova, D. M., Shemetov, A. A., Kaberniuk, A. A. & Verkhusha, V. V. Natural Photoreceptors as a Source of Fluorescent Proteins, Biosensors, and Optogenetic Tools. *Annu. Rev. Biochem.* **84,** 519–550 (2015).
6. Zhang, F. *et al.* The Microbial Opsin Family of Optogenetic Tools. *Cell* **147,** 1446–1457 (2011).
7. Drepper, T. *et al.* Reporter proteins for in vivo fluorescence without oxygen. *Nat. Biotechnol.* **25,** 443–445 (2007).
8. Walter, J. *et al.* Flavin Mononucleotide-Based Fluorescent Proteins Function in Mammalian Cells without Oxygen Requirement. *PLoS One* **7,** e43921 (2012).
9. CRICK, F. Central Dogma of Molecular Biology. *Nature* **227,** 561–563 (1970).
10. Gilbert, W. Origin of life: The RNA world. *Nature* **319,** 618–618 (1986).
11. Kruger, K. *et al.* Self-splicing RNA: Autoexcision and autocyclization of the ribosomal RNA intervening sequence of tetrahymena. *Cell* **31,** 147–157 (1982).
12. Dinger, M. E., Gascoigne, D. K. & Mattick, J. S. The evolution of RNAs with

multiple functions. *Biochimie* **93,** 2013–2018 (2011).

13. Morris, K. V. & Mattick, J. S. The rise of regulatory RNA. *Nat. Rev. Genet.* **15,** 423–437 (2014).
14. Schafer, D. A., Gelles, J., Sheetz, M. P. & Landick, R. Transcription by single molecules of RNA polymerase observed by light microscopy. *Nature* **352,** 444–448 (1991).
15. Maiuri, P. *et al.* Fast transcription rates of RNA polymerase II in human cells. *EMBO Rep.* **12,** 1280–5 (2011).
16. Mandal, M. & Breaker, R. R. Gene regulation by riboswitches. *Nat. Rev. Mol. Cell Biol.* **5,** 451–463 (2004).
17. Winkler, W. C. & Breaker, R. R. REGULATION OF BACTERIAL GENE EXPRESSION BY RIBOSWITCHES. *Annu. Rev. Microbiol.* **59,** 487–517 (2005).
18. Shimoni, Y. *et al.* Regulation of gene expression by small non-coding RNAs: a quantitative view. *Mol. Syst. Biol.* **3,** 138 (2007).
19. Atilho, R. M., Mirihana Arachchilage, G., Greenlee, E. B., Knecht, K. M. & Breaker, R. R. A bacterial riboswitch class for the thiamin precursor HMP-PP employs a terminator-embedded aptamer. *Elife* **8,** (2019).
20. Ames, T. D. & Breaker, R. R. in *The Chemical Biology of Nucleic Acids* 433–454 (John Wiley & Sons, Ltd, 2010). doi:10.1002/9780470664001.ch20
21. McCown, P. J., Corbino, K. A., Stav, S., Sherlock, M. E. & Breaker, R. R. Riboswitch diversity and distribution. *RNA* **23,** 995–1011 (2017).
22. Smith, A. M., Fuchs, R. T., Grundy, F. J. & Henkin, T. Riboswitch RNAs: Regulation of gene expression by direct monitoring of a physiological signal. *RNA*

Biol. **7,** 104–110 (2010).

23. Breaker, R. R. Riboswitches and Translation Control. *Cold Spring Harb. Perspect. Biol.* **10,** a032797 (2018).
24. Serganov, A. & Nudler, E. A decade of riboswitches. *Cell* **152,** 17–24 (2013).
25. Breaker, R. R. Prospects for Riboswitch Discovery and Analysis. *Mol. Cell* **43,** 867–879 (2011).
26. Berens, C., Groher, F. & Suess, B. RNA aptamers as genetic control devices: The potential of riboswitches as synthetic elements for regulating gene expression. *Biotechnol. J.* **10,** 246–257 (2015).
27. Wittmann, A. & Suess, B. Engineered riboswitches: Expanding researchers' toolbox with synthetic RNA regulators. *FEBS Lett.* **586,** 2076–2083 (2012).
28. De Smit, M. H. & Duin, J. Van. Control of Prokaryotic Translational Initiation by mRNA Secondary Structure. *Prog. Nucleic Acid Res. Mol. Biol.* **38,** 1–35 (1990).
29. Bauer, G. & Suess, B. Engineered riboswitches as novel tools in molecular biology. *Journal of Biotechnology* **124,** 4–11 (2006).
30. Cui, C., Shu, W. & Li, P. Fluorescence In situ Hybridization: Cell-Based Genetic Diagnostic and Research Applications. *Front. cell Dev. Biol.* **4,** 89 (2016).
31. Bouhedda, F., Autour, A. & Ryckelynck, M. Light-Up RNA Aptamers and Their Cognate Fluorogens: From Their Development to Their Applications. *Int. J. Mol. Sci.* **19,** (2017).
32. Wang, R. E., Zhang, Y., Cai, J., Cai, W. & Gao, T. Aptamer-based fluorescent biosensors. *Curr. Med. Chem.* **18,** 4175–84 (2011).
33. Paige, J. S., Wu, K. Y. & Jaffrey, S. R. RNA Mimics of Green Fluorescent Protein.

Science (80-.). **333,** 642–646 (2011).

34. Filonov, G. S., Moon, J. D., Svensen, N. & Jaffrey, S. R. Broccoli: Rapid Selection of an RNA Mimic of Green Fluorescent Protein by Fluorescence-Based Selection and Directed Evolution. *J. Am. Chem. Soc.* **136,** 16299–16308 (2014).
35. Dolgosheina, E. V. *et al.* RNA Mango Aptamer-Fluorophore: A Bright, High-Affinity Complex for RNA Labeling and Tracking. *ACS Chem. Biol.* **9,** 2412–2420 (2014).
36. You, M. & Jaffrey, S. R. Structure and Mechanism of RNA Mimics of Green Fluorescent Protein. *Annu. Rev. Biophys.* **44,** 187–206 (2015).
37. Autour, A. *et al.* Fluorogenic RNA Mango aptamers for imaging small non-coding RNAs in mammalian cells. *Nat. Commun.* **9,** 656 (2018).
38. Kellenberger, C. A., Wilson, S. C., Sales-Lee, J. & Hammond, M. C. RNA-Based Fluorescent Biosensors for Live Cell Imaging of Second Messengers Cyclic di-GMP and Cyclic AMP-GMP. *J. Am. Chem. Soc.* **135,** 4906–4909 (2013).
39. Kellenberger, C. A., Hallberg, Z. F. & Hammond, M. C. in *Methods in molecular biology (Clifton, N.J.)* **1316,** 87–103 (2015).
40. You, M., Litke, J. L. & Jaffrey, S. R. Imaging metabolite dynamics in living cells using a Spinach-based riboswitch. *Proc. Natl. Acad. Sci.* **112,** E2756–E2765 (2015).
41. Song, W., Strack, R. L., Svensen, N. & Jaffrey, S. R. Plug-and-Play Fluorophores Extend the Spectral Properties of Spinach. *J. Am. Chem. Soc.* **136,** 1198–1201 (2014).
42. Zhong, W. & Sczepanski, J. T. A Mirror Image Fluorogenic Aptamer Sensor for Live-Cell Imaging of MicroRNAs. *ACS sensors* **4,** 566–570 (2019).

43. Fenno, L., Yizhar, O. & Deisseroth, K. The Development and Application of Optogenetics. *Annu. Rev. Neurosci.* **34,** 389–412 (2011).

44. Christie, J. M., Gawthorne, J., Young, G., Fraser, N. J. & Roe, A. J. LOV to BLUF: Flavoprotein Contributions to the Optogenetic Toolkit. *Mol. Plant* **5,** 533–544 (2012).

45. Möglich, A. & Moffat, K. Engineered photoreceptors as novel optogenetic tools. *Photochem. Photobiol. Sci.* **9,** 1286 (2010).

46. Jäschke, A. Genetically encoded RNA photoswitches as tools for the control of gene expression. *FEBS Lett.* **586,** 2106–2111 (2012).

47. Paige, J. S., Nguyen-Duc, T., Song, W. & Jaffrey, S. R. Fluorescence Imaging of Cellular Metabolites with RNA. *Science (80-.).* **335,** 1194–1194 (2012).

48. Strack, R. L., Song, W. & Jaffrey, S. R. Using Spinach-based sensors for fluorescence imaging of intracellular metabolites and proteins in living bacteria. *Nat. Protoc.* **9,** 146–155 (2013).

49. Kellenberger, C. A. & Hammond, M. C. in *Methods in enzymology* **550,** 147–172 (2015).

50. Rogers, T. A., Andrews, G. E., Jaeger, L. & Grabow, W. W. Fluorescent Monitoring of RNA Assembly and Processing Using the Split-Spinach Aptamer. *ACS Synth. Biol.* **4,** 162–166 (2015).

51. Chang, A. L., Wolf, J. J. & Smolke, C. D. Synthetic RNA switches as a tool for temporal and spatial control over gene expression. *Curr. Opin. Biotechnol.* **23,** 679–688 (2012).

52. Dhamodharan, V., Nomura, Y., Dwidar, M. & Yokobayashi, Y. Optochemical

control of gene expression by photocaged guanine and riboswitches. *Chem. Commun.* **54,** 6181–6183 (2018).

53. Hemphill, J. *et al.* Conditional Control of Alternative Splicing through Light-Triggered Splice-Switching Oligonucleotides. *J. Am. Chem. Soc.* **137,** 3656–3662 (2015).

54. Chaulk, S. & MacMillan, A. M. Caged RNA: photo-control of a ribozyme reaction. *Nucleic Acids Res.* **26,** 3173–3178 (1998).

55. Wulffen, B., Buff, M. C. R., Pofahl, M., Mayer, G. & Heckel, A. Caged glucosamine-6-phosphate for the light-control of riboswitch activity. *Photochem. Photobiol. Sci.* **11,** 489–492 (2012).

56. Walsh, S., Gardner, L., Deiters, A. & Williams, G. J. Intracellular Light-Activation of Riboswitch Activity. doi:10.1002/cbic.201400024

57. Young, D. D., Garner, R. A., Yoder, J. A. & Deiters, A. Light-activation of gene function in mammalian cells via ribozymes. *Chem. Commun. (Camb).* 568–70 (2009). doi:10.1039/b819375d

58. Haller, A., Soulie Re, M. F. & Micura, R. The Dynamic Nature of RNA as Key to Understanding Riboswitch Mechanisms. *Acc. Chem. Res.* **44,** 1339–1348 (2011).

59. Lotz, T. S. *et al.* A light-responsive RNA aptamer for an azobenzene derivative. *Nucleic Acids Res.* (2018). doi:10.1093/nar/gky1225

60. Weber, A. M. *et al.* A blue light receptor that mediates RNA binding and translational regulation. *Nat. Chem. Biol.* (2019). doi:10.1038/s41589-019-0346-y

61. Kowalik, L. & Chen, J. K. Illuminating developmental biology through photochemistry. *Nat. Chem. Biol.* **13,** 587–598 (2017).

62. Matsuda, K. & Irie, M. Diarylethene as a photoswitching unit. *J. Photochem. Photobiol. C Photochem. Rev.* **5,** 169–182 (2004).

63. Kienzler, M. A. *et al.* A Red-Shifted, Fast-Relaxing Azobenzene Photoswitch for Visible Light Control of an Ionotropic Glutamate Receptor. *J. Am. Chem. Soc.* **135,** 17683–17686 (2013).

64. Szymanski, W., Beierle, J. M., Kistemaker, H. A. V, Velema, W. A. & Feringa, B. L. Reversible Photocontrol of Biological Systems by the Incorporation of Molecular Photoswitches Wiktor Szyman sBeierle, J. M., Kistemaker, H. A. V, Velema, W. A., & Feringa, B. L. (2013). Reversible Photocontrol of Biological Systems by the Incorporation of. *Chem. Rev.* **113,** 6114–6178 (2013).

65. You, M. & Jaffrey, S. R. Designing optogenetically controlled RNA for regulating biological systems. *Ann. N. Y. Acad. Sci.* **1352,** 13–19 (2015).

Chapter 2: Regulation of mRNA Translation by a Photoriboswitch

Rotstan, K. A., Abdelsayed, M. M., Passalacqua, L. F. M., Chizzolini, F., Sudarshan, K., Chamberlin, A. R., Míšek, J. & Lupták, A. Regulation of mRNA translation by a photoriboswitch. *Submitted.*

Contribution Statement

A. L. and J. M. designed the study. J. M. and M. M. A. designed the *in vitro* selection experiment. J. M. and K. S. synthesized the ligands with the help of A. R. C. J. M. characterized the ligand. M. M. A. carried out the *in vitro* selection. **K. A. R.** performed the *in vitro* and *in vivo* riboswitch characterization experiments. F. C. and **K. A. R.** designed the luciferase reporter system. L. F. M. P., **K. A. R.**, and M. M. A. performed the structure probing of Were-1. A. L. and **K. A. R.** prepared figures and wrote the manuscript with input from all other authors. **K. A. R.** and M. M. A. authors contributed equally to this work.

2.1 Abstract

Optogenetic tools have revolutionized the study of receptor-mediated biological processes, but such tools are lacking for the study of RNA-controlled systems. To fill this gap, we used *in vitro* selection to isolate a novel RNA that selectively binds the *trans* isoform of a stiff-stilbene (amino-*t*SS), a rapidly and reversibly photoisomerizing small molecule. Structural probing revealed that Were-1 binds amino-*t*SS about 100-times stronger than amino-*c*SS, giving the system robust selectivity for the *trans* isomer. *In vitro* and *in vivo* functional analysis showed that the riboswitch, termed Werewolf-1 (Were-1), inhibits translation of a downstream open reading frame when bound to amino-*t*SS and photoisomerization of the ligand with a sub-millisecond pulse of light induced the protein expression. Similarly, bacterial culture containing the *cis* isoform (amino-*c*SS) supported protein expression, which was inhibited upon photoisomerization to amino-*t*SS. Reversible regulation of gene expression using a genetically encoded light-responsive RNA will broaden the analysis of complex RNA processes in living cells.

2.2 Introduction

Optogenetic techniques have transformed the biomedical sciences by controlling biological events with high spatiotemporal resolution through triggering signal transduction pathways *via* light-sensing proteins[1–4]; however, there are currently no photoactive molecules that can reversibly regulate cellular events at the RNA level. Photo-caged ligands have previously been used to regulate RNA, but their photo-uncaging procedures require relatively long UV light exposure and are irreversible, allowing only a single molecular event to be initiated[5–10]. Furthermore, a light-responsive ribozyme has shown reversible activity[11], and aptamers that bind photo-reversible ligands have been identified[12–14], but these RNAs have only been used *in vitro*. Here we used *in vitro* selection[15–17] to isolate a novel RNA that selectively binds only one photoisoform of a ligand, amino *trans* stiff-stilbene (amino-*t*SS)[18–20]. Chemical probing identified amino-*t*SS–induced RNA structural changes in both the aptamer domain and a downstream expression platform derived from a bacterial riboswitch. *In vitro* and *in vivo* functional analysis showed that the riboswitch, termed Were-1, can induce or inhibit translation of a downstream open reading frame upon exposure to a sub-millisecond pulse of light, through reversible photoisomerization of the ligand. Our results demonstrate how a genetically encoded light-responsive RNA can reversibly regulate gene expression using light, providing a new optogenetic tool to broaden the analysis of complex RNA processes in living cells[20–23].

2.3 Results and Discussion

Photoresponsive synthetic compounds are promising molecules that have potential to optically control RNA conformational changes without harming cellular processes[24,25]. In order to design a ligand capable of binding RNA and directly control gene expression with light, a photoactive ligand was designed and synthesized with the goal of low toxicity, maintaining good cell permeability, good thermal stability of both isomers, and fast optical switching. This ligand, named amino *trans* stiff-stilbene (amino-*t*SS), is a diarylethene compound with an amino group attached by a linker (Fig. 2.1a).

Stilbenes are natural compounds that are synthesized in plants. Their ability to be anti-inflammatory and anti-carcinogenic suggests their non-toxic nature[26]. To obtain good cell permeability, amino-*t*SS contains additional hydroxyl groups in comparison to a commercial *trans* stilbene (*t*S), which enhances the structure's lipophilicity and therefore increases its membrane permeability[27,28]. Furthermore, these hydroxyl groups make amino-*t*SS more soluble in water which is important for experimental purposes. Although the mechanism of isomerization for amino-*t*SS is not yet known, previous studies suggest that upon excitation, stiff-stilbenes convert the energy obtained from an absorbed photon into heat by ultrafast non-adiabatic decay[29,30]. This process accelerates the dissociation of the labile bond, allowing the molecule to switch conformation to its *cis* isoform. The ability of stiff stilbenes to isomerize easily has made them valuable probes for optical switching.

Amino-*t*SS is most stable in the *trans* conformation and is most soluble in DMSO, alike purified amino-*c*SS, but is also relatively stable in water (Supplementary Fig. 2.1d). Using UV-Vis and NMR spectroscopy, it was determined that amino-*t*SS photoisomerizes

to its *cis* isoform at 342 nm and back to the *trans* conformation at 372 nm (Fig. 2.1a-c). The ligand was designed to have a narrow window for photoregulation of both isomerizations in order to keep the rest of the visible spectrum available for the potential readouts of luminescent assays.

To isolate a new aptamer fused to a functional expression platform, we constructed an RNA pool derived from a bacterial SAM-I riboswitch[31] by replacing its ligand-binding domain with a 45-nucleotide random sequence, partially randomizing its anti-terminator and terminator hairpins, and retaining its translation initiation sequences (Supplementary Fig. 2.2). The RNA pool was selected *in vitro* to bind amino-*t*SS coupled to carboxylate agarose beads and eluted under denaturing conditions[16]. We hypothesized that a pool of amino-*t*SS–binding aptamers would include motifs that do not bind the *cis* photoisoform of the ligand and that the *t*SS–binding conformation stabilizes the expression platform in a single state that affects either transcription or translation of a downstream open reading frame (ORF). After six rounds of *in vitro* selection, we cloned the pool into bacterial plasmids and tested individual sequences for amino-*t*SS binding by monitoring RNA–dependent changes in the fluorescence of the amino-*t*SS. One sequence showed markedly increased fluorescence of amino-*t*SS (Supplementary Fig. 2.3, Fig. 2.1c). This sequence, termed Werewolf-1 (Were-1) for its potential light-dependent conformational changes, was chosen for further analysis.

To assess the ligand-dependent structural modulation of Were-1, we performed multiple RNA structure-probing experiments, including digestions with T1 and S1 nucleases[25,26], terbium (III) footprinting[34], in-line probing[35], and selective 2' hydroxyl acylation by primer extension (SHAPE)[36] using a range of amino-*t*SS concentrations (Fig.

2.1b, Supplementary Fig. 2.4). The changes in the pattern of RNA probing suggested that Were-1 undergoes conformational modulation upon introduction of amino-*t*SS in both the sequence derived from the randomized region and the expression platform (Fig. 2.1b, Supplementary Figs. 2.4a–4c, and 2.4g). Control experiments with amino-*t*SS analogs, such as *trans*-stilbene (*t*S), 4,4-*trans*-dihydroxystilbene (*t*DHS), and S-adenosyl methionine (SAM), showed no change in the probing patterns (Supplementary Figs. 2.4c–4f), suggesting that Were-1 is specific for amino-*t*SS. Analysis of the T1 probing experiments revealed a K_D of 1.1 μM, based on the change in band intensity with increasing amino-*t*SS for nucleotide G42, normalized to a control band G72 (Fig. 2.1b). Additionally, a 108-μM K_D was calculated based on the same band intensity change with increasing amino-*c*SS (Supplementary Fig. 2.4g), revealing a 100-fold specificity for the target ligand, amino-*t*SS. The average amino-*t*SS K_D derived from the T1 nuclease probing (at positions 42, 46, 77, and 80; normalized to the band intensity at position 72) was of 1.5 μM, whereas the nuclease S1 probing revealed a K_D of 0.4 μM (based on band intensity change for positions A44-G46), and the terbium (III) footprinting yielded a somewhat higher apparent K_D of 4.8 μM (calculated based on the change in intensity at positions A113 and U107, normalized to G134 control band; Supplementary Fig. 2.4c). In order to establish the location of the amino-*t*SS aptamer domain, we modeled the secondary structure of Were-1 based on the probing data and created mutants hypothesized to affect ligand binding affinity or RNA structural stability (Fig. 2.1c) and tested them *in vitro* and *in vivo*. The secondary structure modeling did not support a conformation containing a Rho-independent transcriptional terminator, in part because

the selected sequence contained two mutations (C90A and U92A), which are predicted to disrupt the stability of a full-length transcription-terminating helix (Fig. 2.1c).

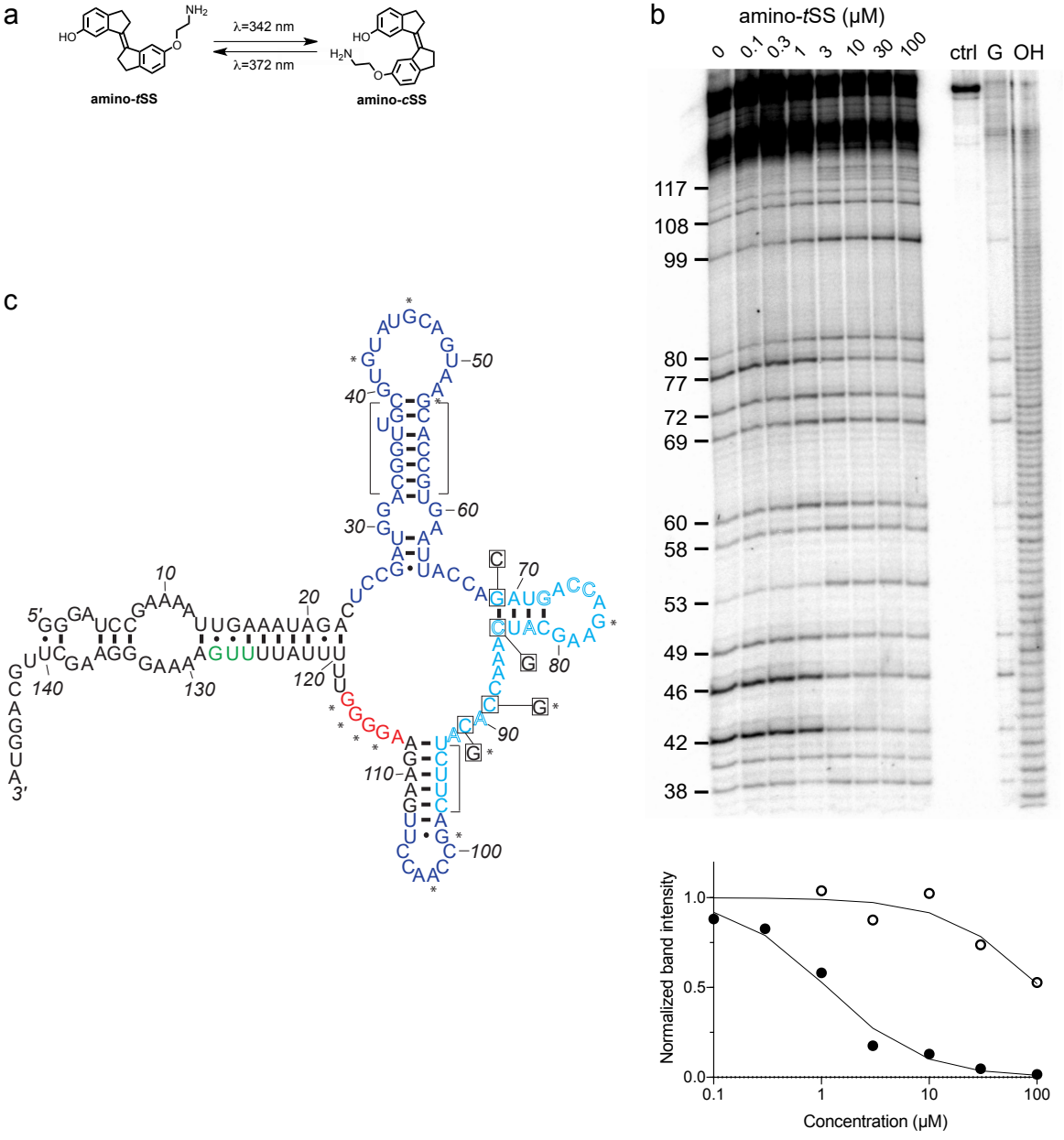

Figure 2.1 | **An amino-*t*SS-responsive aptamer. a**, Amino-*t*SS isomerizes from *trans* to *cis* conformation when exposed to 342 nm light, and back to the *trans* isoform at 372 nm. **b**, RNase T1 probing of Were-1 structure. Right lanes contain a control with undigested RNA (ctrl), a T1-digested sequencing control (G), and a hydroxide-mediated partial digestion ladder (OH) of the RNA. The left lanes show partial T1 digestion in the presence of increasing amino-*t*SS at concentrations indicated above the gel image. The probing shows clear ligand-dependent changes—both increases (e.g. G53, G99, G114-117) and decreases (e.g. G 42, G46, G77)—interspersed throughout the sequence. Below, an apparent K_D of 1.1 μM was calculated based on the change in band intensity with increasing amino-*t*SS (dark, filled circles) for nucleotide G46, normalized to a control band (G72). Additionally, a K_D of 108 μM was calculated based on the change in band intensity with increasing amino-*c*SS (open circles) for the same nucleotide and control (Supplementary Fig. 4g), suggesting high specificity for amino-*t*SS. An average K_D value of 1.5 μM amino-*t*SS was calculated for changes in nucleotides G42, G46, G77, and G80. **c**, Secondary structure prediction of Were-1 derived from all structural probing data in absence of the ligand (see also Supplementary Fig. 4). Partially randomized regions (light blue), the Shine-Dalgarno sequence (red), the start codon (green), and the 3' terminus sequence are derived from the *B. subtilis mswA* SAM-I riboswitch. The 5' part of the aptamer (dark blue) was selected from the random region of the starting pool (Fig. S1). Outlined letters are positions where the selected sequence differs from the *B. subtilis* riboswitch expression platform. Boxed positions were mutated to the indicated nucleotides to identify regions of structural and functional importance. Bracketed regions

indicate areas that do not change in the presence of amino-*t*SS, and asterisks (*) indicate nucleotide positions that do change in the presence of amino-*t*SS.

To test whether Were-1 can directly couple light-induced states of the ligand to the activity of the expression platform *in vitro*, the aptamer was tested for amino-*t*SS–dependent conformational changes using a strand-displacement assay that mimics mRNA binding by the bacterial ribosome[17,37,38]. We designed a DNA duplex in which the longer strand has a toehold sequence corresponding to the reverse complement of the Shine-Dalgarno sequence of Were-1 (Supplementary Table 2.1) and a fluorophore to assess whether the shorter DNA strand, containing a quencher chromophore, is displaced through RNA:DNA hybridization with Were-1 (Supplementary Fig. 2.5a). Polyacrylamide gel electrophoresis (PAGE)-purified Were-1 bound the toehold readily, but the strand displacement was diminished in the presence of amino-*t*SS (Supplementary Fig. 2.5b). Testing the toehold binding at various concentrations of amino-*t*SS revealed a dose dependence with a half–maximal inhibition of toehold binding at ~6 μM (Supplementary Fig. 2.5c).

We next asked whether the ribosome mimic binds this RNA during *in vitro* transcription (Fig. 2.2a, Supplementary Fig. 2.6). In the absence of the ligand, the RNA bound the toehold efficiently, showing a robust increase of fluorescence immediately after transcription initiation. In contrast, the addition of high concentration (14.8 μM) of amino-*t*SS strongly abrogated new binding of the toehold, as revealed by almost a full reduction in the slope of the fluorescence expansion curve (Fig. 2.2b). Intermediate concentrations of amino-*t*SS were tested to assess RNA binding and specificity, yielding a ligand-

dependent response with a half-maximum of ~4 *μ*M amino-*t*SS (Fig. 2.2c). Probing-derived secondary structure modeling of Were-1 suggested substantial ligand-dependent conformational changes in multiple parts of the sequence, except for one predicted hairpin. To confirm the presence of this structural element, we created a variant containing a single mutation (G69C), that was predicted to disrupt this helix, and a presumed compensatory mutant (G69C/C84G) (Fig. 2.1c). The G69C variant showed diminished response to amino-*t*SS, whereas the G69C/C84G double-mutant exhibited partially restored activity, suggesting that these two positions are indeed part of a helix. Other variants, C89G and C91G, designed based on parts of the sequence that showed amino-*t*SS–dependent changes in the structure-probing experiments, both showed decreased sensitivity to the ligand, suggesting that they are essential for ligand binding. Furthermore, when testing toehold binding using the purified *cis* isoform of the stiff stilbene (amino-*c*SS), as well as other stilbenes, such as *t*S, *t*DHS, and *trans* stiff stilbene (*t*SS; Were-1 ligand lacking the aminolated linker), no significant changes in fluorescence were observed (Fig. 2c, Supplementary Fig. 2.7). These results demonstrate that amino-*t*SS stabilizes the RNA in an “OFF” (ribosome-inaccessible) conformation in a dose-dependent manner and with high ligand specificity.

In order to test whether the Were-1 RNA interaction is selective for amino-*t*SS, and potentially acts as an amino-*t*SS riboswitch, we created a construct consisting of the putative riboswitch, including its minor start codon from *Bacillus subtilis* that was present in the starting pool, followed by a firefly luciferase (Fluc) ORF lacking its endogenous start codon. Based on the toehold assays, we hypothesized that in absence of amino-*t*SS, Were-1 would be transcribed in a conformation promoting the translation of the luciferase

enzyme, whereas the presence of amino-*t*SS would stabilize a conformation preventing efficient translation initiation, downregulating the luciferase expression (Fig. 2.2d). Using a purified bacterial *in vitro* transcription/translation system, luciferase production was measured in the presence and absence of amino-*t*SS. In absence of the ligand, the construct exhibited robust luciferase production, demonstrating that the unbound aptamer promotes protein production from a downstream ORF (Fig. 2.2e). In contrast, when amino-*t*SS was added, protein production decreased in a dose-dependent manner (Fig. 2.2f). To confirm that the ligand itself did not impact the *in vitro* translation system, luminescence was tested with a control plasmid lacking the riboswitch, and no amino-*t*SS sensitivity was observed (Supplementary Fig. 2.8).

To further test the riboswitch, we incorporated the construct into a bacterial plasmid and induced its expression in *E. coli* cells (Fig. 2.2g). Bioluminescence, due to luciferase expression and activity, was robust in the absence of ligand, and when the cells were incubated in the presence of amino-*t*SS, bioluminescence was again diminished in a dose-dependent manner (Fig. 2.2h, i). To confirm the specificity of Were-1 for amino-*t*SS, we incubated cells in the presence of amino-*c*SS, *t*S and *t*DHS, and observed no significant change in bioluminescence (Fig. 2.2i). To determine the effect of an alternate start codon on Fluc expression, we changed the UUG start codon in the Were-1-Fluc plasmid to AUG. Bioluminescence was higher in the AUG samples compared to the wild-type UUG construct and showed a similar amino-*t*SS–dependent response (Supplementary Fig. 2.9). Testing the above-mentioned mutants confirmed the G69/C84 interaction, and the importance of the C89 and C91 positions for ligand binding. Taken

together, our results demonstrate that Were-1 controls amino-*t*SS–dependent protein expression *in vitro* and *in vivo,* acting as a translational riboswitch.

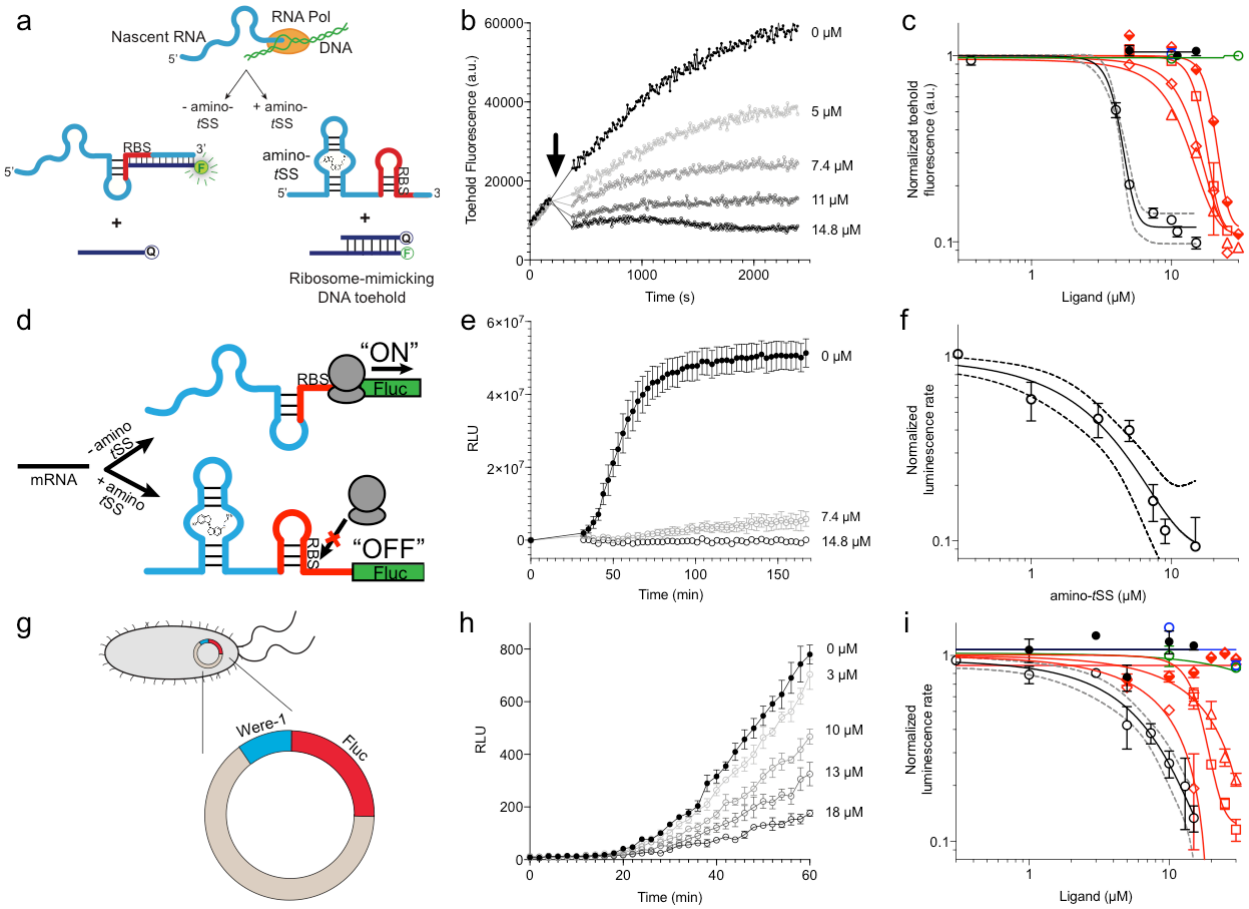

Figure 2.2 | Translation regulation by the Were-1 riboswitch. a, Schematic of co-transcriptional binding of Were-1 RNA to amino-*t*SS in the presence of a toehold-reporter complex. In absence of amino-*t*SS, the transcribed RNA exposes the ribosomal binding site (RBS), enabling binding of the complementary region of the toehold reporter, displacing the quencher strand, and producing a fluorescence signal. In presence of amino-*t*SS, the RNA binds the ligand, sequestering the RBS and preventing displacement

of the quencher strand. **b**, Co-transcriptional response of Were-1 to different concentrations of amino-*t*SS using the toehold reporter. Initial transcriptions of Were-1 without ligand show identical increase in toehold fluorescence for all samples. When amino-*t*SS is added (arrow), a dose-dependent decrease in fluorescence is observed. **c**, Response (± SEM; n=81) of Were-1 (black, open circles), and its variants (red) C89G (triangles), C91G (squares), G69C (half-shaded diamonds), and G69C/C84G (open diamonds), in the presence of amino-*t*SS shows a shift in dose-dependence for single mutations, particularly G69C, and partial recovery of activity for the G69C/C84G double mutant. Were-1 shows no response in the presence of amino-*c*SS (black circles), *trans*-stilbene (green, open circles) and *trans*-4,4-dihydroxystilbene (blue, open circles). **d**, Schematic of amino-*t*SS-dependent inhibition of protein expression *in vitro* using a Were-1-firefly luciferase (Were-1-Fluc) construct. In absence of the ligand, the RBS is exposed and luciferase is translated, whereas in presence of amino-*t*SS, the RBS is sequestered, abrogating Fluc expression. **e**, *In vitro* translation of the Were-1-Fluc construct. Robust luminescence is observed when no ligand is present, but the signal is significantly lower in presence of amino-*t*SS. **f**, Response (± SEM; n = 58) of the Were-1–regulated protein expression to amino-*t*SS. **g**, Schematic of the Were-1-Fluc construct incorporated into a bacterial plasmid. **h**, Were-1–controlled Fluc gene expression in *E. coli*. Bioluminescence is observed in absence of amino-*t*SS, and progressively diminished with increasing amino-*t*SS. **i**, Expression of Were-1-Fluc (± SEM; n=257) *in vivo* (black, open circles), and its variants (red) C89G (triangles), C91G (squares), and G69C/C84G (open diamonds), in the presence of amino-*t*SS, show a dose-dependent response. Were-1 mutant G69C (half-shaded diamond) and Were-1 in the presence of amino-*c*SS (black

circles), *trans*-stilbene (green, open circles) and *trans*-4,4-dihydroxystilbene (blue, open circles) showed no change in bioluminescence, whereas the G69C/C84G double mutant shows restoration of activity similar to wild-type levels. Note, dose-response graphs (**c**, **f**, **i**) are on a log-log scale. The apparent amino-*t*SS IC_{50}s are 3.9 ± 0.2, 2.5 ± 1.0, and 5.3 ± 1.1 μM for the toehold (**c**), *in vitro* translation (**f**), and *in vivo* expression (**i**), respectively. Dashed lines correspond to the 95% confidence interval of the binding model.

We next asked whether Were-1 could regulate gene expression in a light-dependent manner, acting as a photoriboswitch. For this to occur, the *trans* isoform of the stiff stilbene must photoisomerize to its *cis* state, preventing binding of the Were-1 aptamer domain, and promoting expression of a downstream ORF.

Riboswitches are sensitive to co-transcriptional events because they are capable of adopting different RNA folds as they are transcribed by RNA polymerase [39]. To first monitor changes in RNA folding over time, we used the toehold-fluorophore system to determine whether the DNA duplex was in a bound state (no strand displacement) versus an unbound state (strand displacement releasing the quencher DNA, yielding fluorescence) during transcription. Our results show that when the amino-*t*SS-bound Were-1 structure was irradiated at 342 nm of light, the toehold fluorescence increased, suggesting that the RNA increased the binding to the ribosome mimic present on the DNA toehold. Furthermore, when exciting amino-*c*SS at 372 nm of light to switch the ligand to its *trans* isoform, we observed a decrease in toehold fluorescence growth, indicating that the photo-generated amino-*t*SS was able to re-bind the Were-1 RNA. The irradiation was repeated until all toehold was bound, with each switch showing consistent results

(Supplementary Fig. 2.10). This experiment shows reversible, wavelength-dependent binding of the ribosome mimic, emulating light-dependent protein expression from a downstream open reading frame.

To study the system further, we used the Were-1-luciferase construct and the purified bacterial *in vitro* transcription/translation system to test whether luciferase expression could be regulated by our putative photoriboswitch. We found that when the reaction was irradiated at 342 nm of light, luminescence increased, suggesting that Were-1's conformation changed to expose the RBS, enabling luciferase expression. When the *cis* stilbene was photoisomerized to the *trans* state (amino-*t*SS) at 372 nm of light, luciferase protein production slightly decreased (Supplementary Fig. 2.11). These data are consistent with an *in vitro* activity of a photoriboswitch.

Finally, we used *E. coli* containing the Were-1-Fluc construct to determine whether gene expression can be regulated with a pulse of light. As shown above, bioluminescence was greatly diminished in the presence of amino-*t*SS (Fig. 2.2i). Upon exposing the bacteria to 342 nm light, we saw a robust increase in bioluminescence (Fig. 2.3a, b and Supplementary Fig. 2.12). This result strongly suggests that upon photoisomerization of amino-*t*SS to the *cis* isoform with a pulse of light, Were-1 was able to change conformation and expose its RBS to allow luciferase production. To confirm these results, we performed control experiments, in which cells were covered during the excitation to distinguish between regular *E. coli* growth behavior and the increase in bioluminescence from the riboswitch (Fig. 2.3a, b). Additionally, in another experiment, we excited cells with a different wavelength of light (500 nm) that should not impact the isomerization of the ligand (Supplementary Fig. 2.12). Both controls showed lower bioluminescence

compared to the 342 nm excited samples. To further analyze the system, we tested the temporal dependence of Were-1–regulated Fluc production by exposing an amino-*t*SS–containing bacterial culture to 342 nm light for various lengths of time. Relative to controls that were unexposed, the highest luciferase expression was seen at an exposure time of 500 *μ*s (Fig. 2.3b). Furthermore, when testing the same system using amino-*c*SS, bioluminescence decreased in a dose-dependent manner with increasing amino-*c*SS concentration after exposure to 390 nm light (Fig. 2.3c). This result strongly suggests that by isomerizing amino-*c*SS to its *trans* isoform with a pulse of light, Were-1 was able to sequester its RBS to inhibit luciferase production. Testing the temporal response of Were-1–regulated Fluc expression in the presence of amino-*c*SS revealed that Were-1 regulates expression optimally at short exposures, showing the highest inhibition after a millisecond of light exposure (Fig. 2.3d). Based on isomerization data (Supplementary Fig. 2.2b), this effect is likely due to the ligand reaching a semi-photostationary state after longer light exposure. No difference in cell density was observed among the experiments, implying that neither the ligand, nor the light pulses affect the bacterial growth, and suggesting negligible photo-damage to the cells.

We next asked whether Were-1 could reversibly regulate gene expression *in vivo*, providing the first optogenetic tool to reversibly regulate cellular events at the RNA level. Using the same *E. coli* construct, we measured bioluminescence over two hours in samples that were covered during excitations, and therefore unexposed to light, samples that were exposed to a millisecond of 342 nm light, and samples that were exposed to 342 nm and then later excited at 390 nm for a sub-millisecond. Initial values prior to excitation showed no significant difference in bioluminescence twenty-five minutes post

induction (Fig. 2.3e). Samples that were then exposed to 342-nm light showed a significant increase in luciferase expression forty-five minutes after exposure, compared to the unexposed control. Lastly, the samples that were subsequently exposed to 390-nm light decreased in bioluminescence forty-five minutes post exposure in comparison to those that were unexposed and those that were exposed only to 342 nm. As an additional control, the G69C mutant was exposed alongside Were-1 and showed no significant difference when G69C excited with 342 nm light, or 342 nm and 390 nm (Fig. 2.3f). These results strongly suggest that Were-1 is a photoriboswitch that can reversibly regulate protein expression *in vivo*.

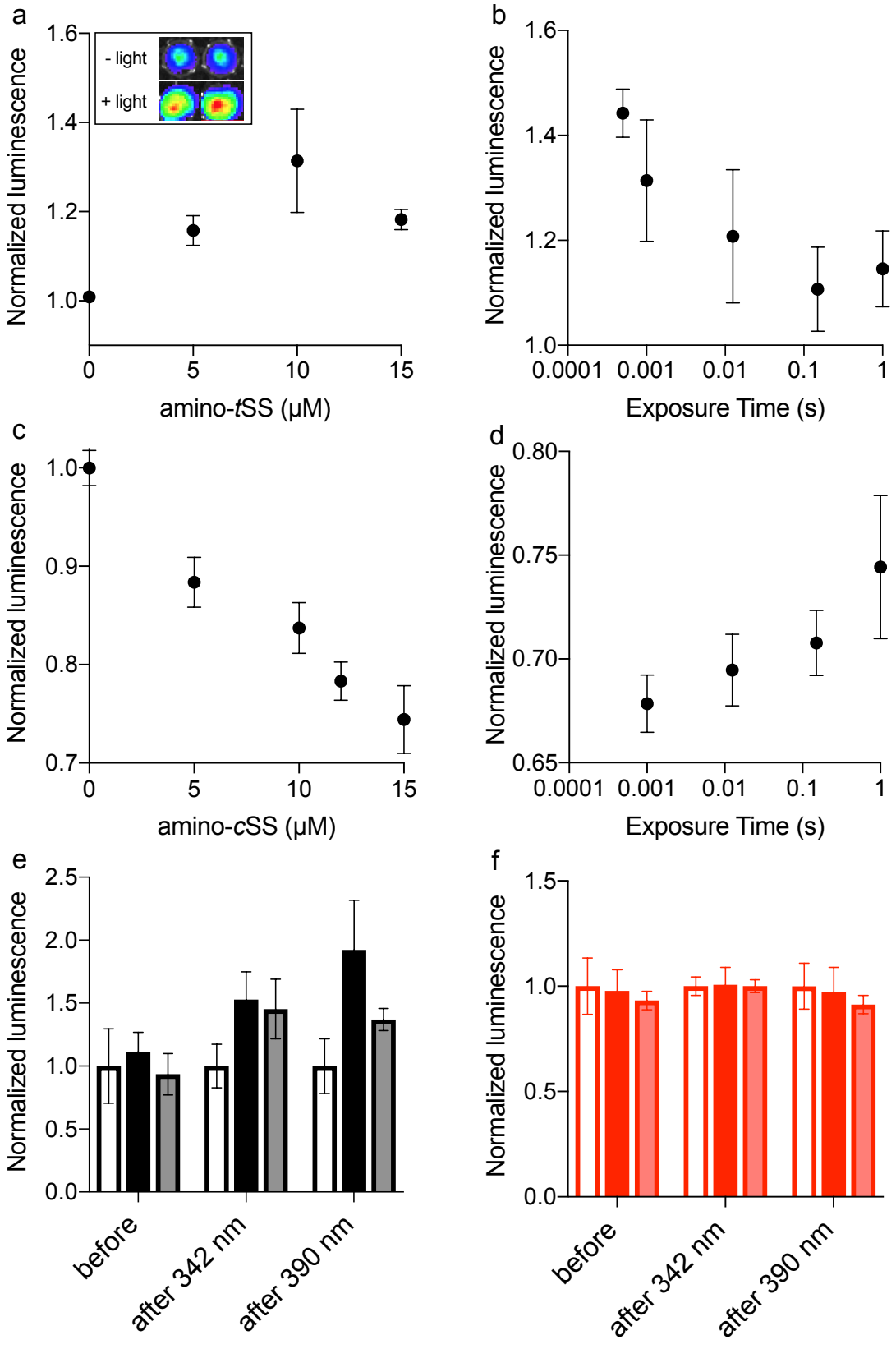
a
Normalized luminescence
1.6
1.4
1.2
1.0
- light
+ light
0
5
10
15
amino-tSS (μM)
b
Normalized luminescence
1.6
1.4
1.2
1.0
0.0001
0.001
0.01
0.1
1
Exposure Time (s)
c
Normalized luminescence
1.0
0.9
0.8
0.7
0
5
10
15
amino-cSS (μM)
d
Normalized luminescence
0.80
0.75
0.70
0.65
0.0001
0.001
0.01
0.1
1
Exposure Time (s)
e
Normalized luminescence
2.5
2.0
1.5
1.0
0.5
0.0
before
after 342 nm
after 390 nm
f
Normalized luminescence
1.5
1.0
0.5
0.0
before
after 342 nm
after 390 nm

Figure 2.3 | **Regulation of luciferase expression by the Were-1 photoriboswitch *in vivo*. a**, Normalized amino-*t*SS–dependent bioluminescence (± SEM) of the Were-1-Fluc construct after 1 ms exposure of 342 ± 5 nm light (Φ_q = 1.4*10^{-2} W/cm^2). The largest change in expression was observed in the presence of 10 μM amino-*t*SS. Inset shows the light–dependent bioluminescence of the bacterial cultures at 10 μM ligand. **b**, Were-1 regulation of luciferase expression (± SEM) *in vivo* at various exposure times in presence of 10 μM amino-*t*SS. **c**, Normalized bioluminescence of the Were-1-Fluc *E. coli* incubated with amino-*c*SS after 1 s exposure of 390 ± 9 nm light (Φ_q = 5.5*10^{-2} W/cm^2) showing progressively higher protein expression inhibition at higher amino-*c*SS concentrations, presumably due to higher concentration of amino-*t*SS after photoisomerization. **d**, Change of Fluc expression after photoisomerization of 15 μM amino-*c*SS at 390 ± 9 nm light for various exposure times, showing largest photoswitching at 1 ms exposure. **e,** Regulation of luciferase expression (± SEM) by the Were-1-Fluc construct before exposure, forty-five minutes after a 1-ms pulse of 342 ± 5 nm light (dark and gray), which resulted in increased bioluminescence compared to control (clear), and forty-five minutes after 0.5 ms of 390 ± 9 nm exposure that resulted in decreased bioluminescence (gray) compared to samples that were only exposed to 342 nm. **f,** Luciferase expression (± SEM) by the Were-1-Fluc G69C mutant using the same conditions as above (e), showing no significant change in expression after exposure to 342 nm (red, light red) or 342 nm and 390 nm (light red) compared to unexposed controls (clear).

2.4 Conclusion

Taken together, we show that novel riboswitches, regulated by synthetic ligands, can be evolved from random libraries fused to expression platforms. In the case of Were-1, binding of the target ligand stabilizes the RNA in a conformation that impedes the translation of a downstream ORF. This approach will likely also yield transcription-regulating riboswitches, and further molecular engineering will allow regulation of a wide range of cellular events in both *cis* and *trans*. We expect that Were-1 and similar photoriboswitches will allow reversible photoregulation of a variety of RNA-centered cellular events with a very high spatiotemporal resolution in bacteria and multicellular organisms alike.

2.5 Materials and Methods

Reagents and equipment. Unless otherwise stated, all reagents were purchased from Sigma-Aldrich. (E)-6'-(2-aminoethoxy)-2,2',3,3' tetrahydro-[1,1'-biindenylidene]-6-ol (amino-*t*SS) was synthesized and prepared as described below. Commercially available reagents were used without further purification. Absorbance spectra were recorded with a Thermo Scientific NanoDrop 1000 spectrophotometer. Fluorescence excitation and emission spectra were measured with a Varian Cary Eclipse fluorescence spectrometer, unless otherwise specified. Bioluminescence was measured using an Andor 866 EMCDD camera, BioTek Synergy H1 plate reader, or IVIS Lumina II.

Synthesis of (E)-6'-(2-aminoethoxy)-2,2',3,3' tetrahydro-[1,1'-biindenylidene]-6-ol. All starting reagents were commercially available, and of analytical purity, and were used without further treatment. Solvents were dried according to standard methods. ^{1}H and spectra were recorded on Varian UNITY INOVA-300 and Bruker Avance-600 instruments. Chemical shifts (δ) are reported in ppm relative to residual solvent peak (DMSO: δ_H = 2.50 ppm) as internal standard. Accurate mass measurements (HRMS) were obtained by ESI on an Agilent 6530 Q-TOF MS spectrometer. Analytical TLC was performed using a precoated silica gel 60 Å F_{254} plates (0.2 mm thickness) visualized with UV at 254 nm. Preparative column chromatography was carried out using silica gel 60 Å (particle size 0.063–0.200 mm). Purifications by HPLC were performed under the following conditions: Agilent ZORBAX SB-C18 column (5 µL, 9.4x150 mm); UV/Vis detection at λ_{obs} = 254 nm; flow rate 4 mL/min; gradient elution method H_2O (0.1 % TFA) – CH_3CN (0.1 % TFA) from 95:5 to 0:100 in 20 min. Purity of compounds was confirmed using Agilent eclipse plus

C18 column (3.5 µL, 4.6x100 mm); UV/Vis detection at λ_{obs} = 254 nm; flow rate 0.5 mL/min; gradient elution method H_2O (0.1 % TFA) – CH_3CN (0.1 % TFA) from 95:5 to 0:100 in 20 min.

Synthesis details

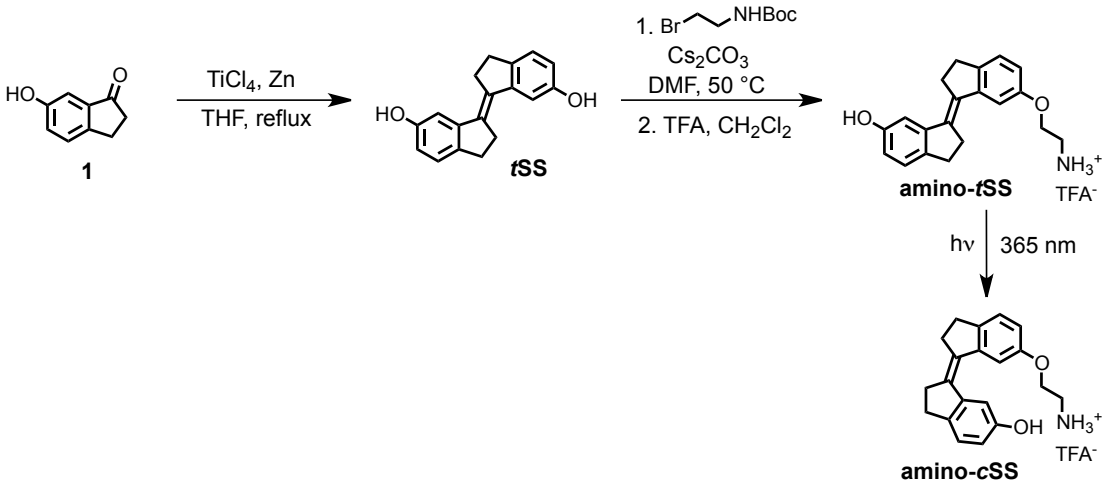

Scheme S1. Synthesis of stiff stilbene derivatives ***t*SS, amino-*t*SS,** and **amino-*c*SS**.

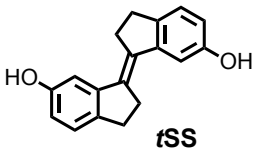

(*E*)-2,2',3,3'-tetrahydro-[1,1'-biindenylidene]-6,6'-diol (*t*SS). To a stirred suspension of zinc powder (3.20 g, 48.92 mmol) in dry THF (50 ml), $TiCl_4$ (4.67 g, 24.58 mmol) was added over 10 minutes at 0 °C. The resulting slurry was heated at reflux for 1.5 h. Then a THF solution (50 ml) of indanone **1** (600 mg, 4.05 mmol) was added over 3 h period by syringe pump to the refluxing mixture. The reflux was continued for 30 minutes after the addition was complete. After cooling to room temperature, the reaction mixture was

poured into a saturated solution of NH_4Cl and extracted with CH_2Cl_2. The organic solutions were dried over $MgSO_4$ and concentrated by rotary evaporation under reduced pressure. The crude product was purified by column chromatography using silica gel (hexane/iPrOH = 10:0.5) to afford ***t*SS** in 51 % yield (273 mg) as a white solid. ^{1}H NMR (400 MHz, DMSO-d_6): δ 2.95 (m, 4H), 3.02 (m, 4H), 6.63 (dd, J = 8.1, 2.2 Hz, 2H), 7.02 (d, J = 2.3 Hz, 2H), 7.11 (d, J = 8.0 Hz, 2H), 9.17 (s, 2H). ^{13}C NMR (100 MHz, DMSO-d_6): δ 29.6, 31.9, 111.0, 114.5, 125.2, 135.0, 137.0, 143.7, 156.1. HRMS (ESI): *m/z* $[M]^+$ calculated for $C_{18}H_{16}O_2$ 264.1145; found: 264.1141.

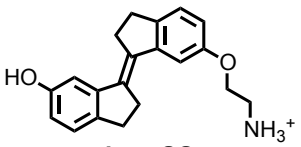

amino-*t*SS

***E*)-6'-(2-aminoethoxy)-2,2',3,3'-tetrahydro-[1,1'-biindenylidene]-6-ol (amino-*t*SS).** A mixture of ***t*SS** (125 mg, 0.47 mmol), 2-(Boc-amino)ethyl bromide (106 mg, 0.47 mmol), Cs_2CO_3 (772 mg , 2.37 mmol) and *n*Bu_4NBr (6 mg, 0.02 mmol) in DMF (15 ml) was heated at 50 °C for 6 h. After cooling to room temperature, CH_2Cl_2 was added and the mixture was washed with a saturated solution of NH_4Cl, water, brine and dried over $MgSO_4$. The organic solutions were concentrated by rotary evaporation under reduced pressure. The crude product was dissolved in a mixture of CH_2Cl_2/TFA (16 ml; 3:1) and stirred at room temperature for 30 minutes. The reaction mixture was concentrated by rotary evaporation under reduced pressure and purified by HPLC (gradient elution method H_2O (0.1 % TFA) – CH_3CN (0.1 % TFA) from 95:5 to 0:100) to afford **amino-*t*SS** (as a TFA salt) in 42 % yield (84 mg) as an off-white solid. ^{1}H NMR (400 MHz, DMSO-d_6): δ 2.96 (m, 4H), 3.01

(m, 4H), 3.22 (t, *J* = 5.1 Hz, 2H), 4.17 (t, *J* = 5.1 Hz, 2H), 6.66 (dd, *J* = 8.1, 2.2 Hz, 1H), 6.87 (dd, *J* = 8.2, 2.3 Hz, 1H), 7.03 (d, *J* = 2.2 Hz, 1H), 7.13 (d, *J* = 8.1 Hz, 1H), 7.16 (d, *J* = 2.4 Hz, 1H), 7.27 (d, *J* = 8.3 Hz, 1H), 8.10 (s, 3H), 9.28 (s, 1H). ^{13}C NMR (100 MHz, DMSO-d_6): δ 29.58, 29.64, 31.8, 31.9, 38.5, 54.7, 110.8, 111.1, 113.6, 114.8, 125.3, 125.4, 134.5, 135.9, 137.1, 139.6, 143.6, 144.0, 156.2, 156.9. HRMS (ESI): *m/z* $[M+H]^+$ calculated for $C_{20}H_{21}NO_2$ 308.1645; found: 308.1651.

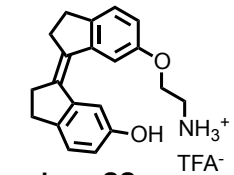

amino-*c*SS

***(Z)*-6'-(2-aminoethoxy)-2,2',3,3'-tetrahydro-[1,1'-biindenylidene]-6-ol ((Z)-1; amino-*c*SS).** A solution of **amino-*t*SS** (15 mg, 35.6 µmol) in DMSO (1 ml) in NMR cuvette was irradiated with handheld UV lamp (8 W) for 15 min. The resulting mixture of **amino-*t*SS** and **amino-*c*SS** was purified by HPLC (gradient elution method H_2O (0.1 % TFA) – CH_3CN (0.1 % TFA) from 95:5 to 0:100) to afford **amino-*c*SS** (as a TFA salt) in 20 % yield (2 mg) as an off-white solid. ^{1}H NMR (400 MHz, DMSO-d_6): δ 2.75 (m, 4H), 2.85 (m, 4H), 3.22 (t, *J* = 5.1 Hz, 2H), 4.13 (t, *J* = 5.1 Hz, 2H), 6.63 (dd, *J* = 8.2, 2.2 Hz, 1H), 6.84 (dd, *J* = 8.2, 2.2 Hz, 1H), 7.12 (d, *J* = 8.2 Hz, 1H), 7.25 (d, *J* = 8.3 Hz, 1H), 7.40 (d, *J* = 2.0 Hz, 1H), 7.53 (d, *J* = 2.0 Hz, 1H), 8.02 (s, 3H), 9.25 (s, 1H). ^{13}C NMR (100 MHz, DMSO-d_6): δ 29.2, 29.3, 34.9, 35.0, 38.5, 64.4, 108.9, 109.4, 114.5, 115.2, 125.8, 125.9, 134.4, 135.7, 138.6, 140.79, 140.84, 141.1, 155.46, 156.1. HRMS (ESI): *m/z* $[M+H]^+$ calcd for $C_{20}H_{21}NO_2$ 308.1645; found: 308.1644.

***In vitro* RNA transcription**. RNA was transcribed at 37 ˚C for one hour in a 50 µL volume containing 40 mM tris-HCl, 6 mM dithiothreitol (DTT), 2 mM spermidine, 1.25 mM each rNTP, 8 mM $MgCl_2$, 1 unit of T7 RNA polymerase, and 5 pmol of DNA template. The transcripts were purified by 10 % PAGE under denaturing conditions (7 M urea). RNA was eluted from the gel into 300 µL of 300 mM KCl and precipitated by adding 700 µL of 95 % ethanol at –20 °C.

***In vitro* selection of amino-*t*SS aptamers.** An RNA pool derived from a *B. subtilis mswA* SAM-1 riboswitch, located in the 5′ untranslated region of the *metI* (cystathionine gamma-synthase, also denoted as *yjcI*) gene [31,40] was designed by replacing the riboswitch ligand-binding domain with a random region of 45 nucleotides. The anti-terminator stem and upstream half of the transcriptional terminator sequence were partially randomized at a 15 % level, and the loop of the terminator stem was fully randomized. The remaining part of the riboswitch, including the downstream half of the transcriptional terminator stem, containing a ribosome binding site (RBS) that binds the 3' end of *B. subtilis* 16S rRNA (3'-UUUCCUCCACUAG-5') [41] and an alternative UUG start codon, was retained (Supplementary Fig. 1). The pool was synthesized by Yale School of Medicine's Keck Oligonucleotide Synthesis facility as a single template strand that was then purified by 10 % PAGE and converted into dsDNA by a primer-extension reaction using a primer corresponding to the T7 RNA polymerase promoter. The pool was transcribed at an estimated sequence diversity of 10^{15}.

From that pool, RNAs were selected to bind amino-*t*SS, as follows. PAGE-purified ^{32}P-labeled RNA transcripts of the pool were precipitated, dried, and resuspended in a solution containing 140 mM KCl, 10 mM NaCl, 10 mM tris-chloride, pH 7.5, and 5 mM $MgCl_2$ (binding buffer). The RNA mixture was heated to 70 °C for three minutes and loaded onto agarose beads for a counter-selection step. Binders were discarded and the flow-through was incubated on agarose beads linked to amino-*t*SS. The beads were shaken for five minutes at room temperature, and the unbound RNA was collected. Amino-*t*SS beads were then washed with binding buffer for five minutes at room temperature. This washing step was repeated six times. Potential aptamers were then eluted twice with denaturing buffer, consisting of 7 M urea and 5 mM ethylenediaminetetraacetic acid (EDTA) in 45 mM tris, 45 mM borate buffer, pH 8, and heated at 95 °C for five minutes. Each fraction was analyzed for radioactivity using a liquid scintillation counter. Elutions were pooled, precipitated, dried, and resuspended in water for reverse transcription. The pool was reverse transcribed, and the cDNA was amplified by PCR and used for the next round of selection.

Screening of potential amino-*t*SS binders. After six rounds of *in vitro* selection, the selected pool was cloned into a TOPO TA plasmid (Invitrogen) and transformed into DH5α *E. coli* cells. Cells were plated on agar containing kanamycin and incubated overnight at 37 ˚C. Individual colonies were picked from the master plate and inoculated overnight in Luria Broth containing kanamycin. Plasmids were extracted and purified using a Miniprep Kit (QIAGEN), and sequenced (GENEWIZ). Individual clones were PCR-amplified using the library-specific primers and transcribed to test their optical activity in

the presence and absence of amino-*t*SS. *t*SS emission spectra were collected using an excitation at 355 nm. Were-1 showed the highest increase in amino-*t*SS fluorescence at 430 nm and was chosen for further analysis.

Structure probing of Were-1.

T1 nuclease probing. Were-1 RNA was dephosphorylated in a solution of the reaction buffer (50 mM potassium acetate, 20 mM Tris-acetate, 10 mM magnesium acetate, 100 µg/ml BSA, pH 7.9), 1 µg of purified RNA, and 1.5 unit of Shrimp Alkaline Phosphatase (NEB). The reaction was incubated at 37 °C for 30 minutes, and heat-inactivated at 65 °C for 5 minutes.

5′–labeled RNA (8000 cpm) was prepared in reaction buffer (70 mM Tris-HCl, pH 7.6, 10 mM $MgCl_2$, 5 mM DTT) using 1 µg of 5′–dephosphorylated RNA, 2 µCi [γ-^{32}P] ATP (Perkin Elmer), and 15 units of T4 PNK enzyme (NEB). The reaction was incubated at 37 °C for two hours and PAGE–purified.

The 5′–labeled Were-1 RNA was added into binding buffer and the indicated concentrations of amino-*t*SS or controls (no ligand, amino-*c*SS, tS, tDHS, and SAM), and were incubated at 55 °C for 5 minutes and subsequently cooled at room temperature for 5 minutes. Next, T1 nuclease was added (0.05 units; Thermo Fisher Scientific) and samples were incubated at 37 °C for 15 minutes. All conditions were then quenched with a mixture of 7 M urea and 10 mM EDTA. Afterwards, the RNA was added to an equal volume of phenol:chloroform:isoamyl alcohol (25:24:1) and vortexed. Samples were

centrifuged for 3 minutes at 8,000 RPM, and the aqueous phase was collected and transferred to a new tube. Samples were fractionated on a 10% PAGE gel and exposed to a phosphor image screen (GE Healthcare) for a minimum of 24 hours. The screen was scanned on a GE Typhoon phosphor imager.

A guanosine-specific sequencing lane was resolved in parallel to all samples using 5′–labeled or 3′–labeled RNA (8000 cpm*)*, as specified, in T1 digestion buffer (250 mM sodium citrate, pH 7) and 0.5 units T1. Reactions were incubated at 55 °C for 5 minutes and quenched with a solution containing 7 M urea and 10 mM EDTA. RNA was extracted using phenol-chloroform, as noted above. Partial alkaline hydrolysis was also resolved in parallel by adding 5′–labeled or 3′–labeled RNA (8000 cpm), as specified, into a hydrolysis buffer (50 mM $NaHCO_3$, 1 mM EDTA, pH 10). Reactions were incubated at 95 °C for 10 minutes and quenched in a solution containing 7 M Urea and 10 mM EDTA. RNA was extracted using phenol-chloroform.

SHAPE. A selective 2'-hydroxyl acylation and primer extension **(**SHAPE) reaction, as described [42], was carried out on Were-1 in the presence of increasing amino-*t*SS concentrations and 30 μM controls (amino-*c*SS, tDHS, tS, and SAM).

S1 nuclease probing. Reactions were prepared by adding 3′–labeled Were-1 RNA (8000 cpm) into S1 nuclease buffer (40 mM sodium acetate, pH 4.5, 300 mM NaCl, and 2 mM $ZnSO_4$), and the indicated concentrations of amino-*t*SS, and were incubated at 55 °C for 5 minutes and subsequently cooled at room temperature for 5 minutes. Next, S1 nuclease

was added (0.2 units; Thermo Fisher Scientific) and samples were incubated at 37 °C for 10 minutes and quenched in a solution of 7 M Urea and 10 mM EDTA. Samples were extracted using phenol-chloroform and resolved on a denaturing 10 % PAGE gel. The gel was then exposed to a phosphor image screen and scanned on a GE Typhoon phosphor imager. The sequences in the degradation pattern were assigned by running T1 digestion and partial alkaline hydrolysis in parallel lanes, as noted above.

Terbium (III) footprinting. Reactions were prepared by adding 5′–labeled Were-1 RNA (8000 cpm) into the binding buffer, and the indicated concentrations of amino-*t*SS or controls (no ligand, amino-*c*SS, tS, tDHS, and SAM), and were incubated at 55 °C for 5 minutes and subsequently cooled at room temperature for 5 minutes. Terbium (III) chloride was added to a final concentration of 10 mM and samples were incubated at 37 °C for 30 minutes and then quenched with a solution of 7 M urea and 10 mM diethylenetriaminepentaacetic acid (DTPA). Were-1 RNA was extracted using phenol-chloroform, as noted above, and samples were fractionated on a denaturing 10 % PAGE gel. The gel was exposed to a phosphor image screen (GE Healthcare) and scanned on a GE Typhoon phosphor imager. The sequences in the degradation pattern were assigned by running TI digestion and partial alkaline hydrolysis in parallel lanes, as noted above.

In–line probing. Reactions were prepared by adding 3′–labeled RNA (8000 cpm) into the binding buffer, pH 8.5, and the indicated concentrations of controls (no ligand, cSS, tS, tDHS, and SAM). Samples were initially incubated at 55 °C for 5 minutes and then

cooled at room temperature for 5 minutes, and then incubated at 37 °C for 20 hours. All conditions were quenched in a solution of 7 M Urea and 10 mM EDTA. Were-1 RNA was extracted using phenol-chloroform, as noted above, and run on a denaturing 10 % PAGE gel. The gel was exposed to a phosphor image screen (GE Healthcare), and scanned on a GE Typhoon phosphor imager. The sequences in the degradation pattern were assigned by running T1 digestion and alkaline hydrolysis in parallel lanes, as noted above.

All gels were analyzed in ImageJ. Structure predictions of Were-1 in the absence of amino-*t*SS were performed using RNAfold of the Vienna RNA package [43] (Fig. 1c).

***In vitro* strand displacement reaction.** A dsDNA reporter was designed to contain a toehold that complements the Shine-Dalgarno sequence of the riboswitch, in which the longer (toehold) strand (Rep F) contained the 3' toehold sequence, a reverse complement of the Shine-Dalgarno sequence, as well as a 5' fluorescein. The shorter strand (Rep Q) contained a 3' Iowa black quencher (Supplementary Table 1). A solution of 2:1 Rep Q:Rep F oligos in binding buffer was incubated at 95 °C for 1 minute, followed by 25 °C for 5 minutes, to anneal the strands and form the dsDNA reporter construct.

In a Falcon 384-well Optilux Flat Bottom plate, strand displacement was initiated by adding 100 nM of purified Were-1 RNA to 50 nM of toehold-fluorophore reporter. Amino-*t*SS was quickly added to some samples to test for ligand-dependent displacement. Fluorescence emission was recorded in a BioTek Synergy plate reader over a 45-minute

period under continuous illumination using the following parameters: excitation wavelength, 485 nm; emission wavelength, 520 nm.

***In vitro* co–transcriptional toehold-binding kinetics of Were-1**. *In vitro* transcription was performed similarly to the above–described RNA transcription assay with the following modifications: 3 pmol template DNA and 50 nM toehold-fluorophore reporter were used. A 30 µL transcription reaction was initiated by the addition of 4 mM rNTP mix (containing 1mM of each rNTP) and fluorescence emission of the toehold-fluorophore reporter was recorded in a Varian Cary Eclipse fluorimeter under continuous illumination at 37 °C using the following parameters: excitation wavelength, 485 nm; emission wavelength, 520 nm; increment of data point collection, 0.01 s; slit widths, 10 nm. These conditions were used for the entire experiment unless stated otherwise. After an initial fluorescence increase, corresponding to the initial burst of transcription, amino-*t*SS was rapidly added to the solution and fluorescence emission was recorded for 200 s. To switch amino-*t*SS to the *cis* isoform (amino-*c*SS), the solution was excited at 342 nm (slit width, 2.5 nm; $\Phi_q = 6.8*10^{-5}$ W/cm^2) for 60 s. Fluorescence emission of the toehold-fluorophore reporter was again recorded for 200 s. To switch the *cis* isoform back to the *trans* state, the solution was excited at 372 nm (slit width, 2.5 nm; $\Phi_q = 10*10^{-5}$ W/cm^2) for 60 s. Again, fluorescence emission of the toehold-fluorophore reporter was recorded for 200 s. This process was repeated two to three more times until fluorescence plateaued.

IC_{50} measurements. A dose-response of the Were-1 riboswitch to the target ligand (amino-*t*SS) was assessed by measuring fluorescence as a function of ligand

concentration in the presence of a toehold-fluorophore reporter construct (50 nM). Fluorescence emission was recorded under continuous illumination at 37 °C using the following parameters: excitation wavelength, 485 nm; emission wavelength, 520 nm; increment of data point collection, 0.01 s; slit widths, 10 nm. The apparent rate constants were measured and plotted against the amino-*t*SS concentrations (or other ligands, as specified). The data were normalized to the no-amino-*t*SS control. The IC_{50} was extracted from fitting a curve to the graph using the equation:

$$\text{Normalized fluorescence} = 1 - \frac{[\text{ligand}]}{[\text{ligand}] + IC_{50}}$$

***In vitro* co–transcriptional magnesium dependence of Were-1 toehold-binding.** Using the same conditions as above, the fluorescence response of toehold-binding to the Were-1 riboswitch in the presence of 8.4 μM amino-*t*SS under various Mg^{2+} concentrations was measured. Fluorescence emission was recorded under continuous illumination at 37 °C on a BioTek Synergy H1 plate reader.

Cloning the Were-1 riboswitch for expression in *E. coli* cells. Were-1 DNA was cloned into the pBV-Luc (Addgene) vector in order to obtain a fused riboswitch-firefly luciferase (Fluc) reporter construct. The PCR primers were designed to add a 5' *EcoRI* site to the template Were-1 DNA upstream of the T7 promoter and a 3' overhang containing 35 nucleotides of the Fluc gene directly downstream of its start codon to replace the Fluc start codon sequence. Both the PCR product and plasmid were digested by *EcoRI HF* and *KasI* (New England BioLabs) and purified. The purified construct was

then inserted at the 5' end of the Fluc coding sequence with T4 DNA ligase (New England BioLabs). The resulting vector was termed Were-1-Fluc (Table 1).

Were-1-Fluc was transformed into DH5α *E. coli* cells and grown overnight on agar plates containing ampicillin at 37 °C. Ten colonies were picked from a master plate and individual clones were inoculated overnight in Luria Broth containing ampicillin. Plasmids were purified using a Miniprep Kit (QIAGEN) and individually sequenced (GENEWIZ). Correct constructs were transcribed *in vitro* and fractionated on an agarose gel to confirm sequencing results by measuring the size of the fused construct. Using the same procedure as above, one clone was analyzed in an *in vitro* co-transcriptional toehold-binding experiment to test whether the new fused construct was able to function similarly to the stand-alone riboswitch.

***In vitro* transcription and translation kinetics.** The PURExpress *in vitro* protein synthesis kit (New England BioLabs) was used to transcribe and translate Were-1-Fluc. Experiments were performed similarly to the kit assay conditions with the following modifications: 200 ng/μL DNA, 100 μM D-luciferin, and 2 mM $MgCl_2$. Amino-*t*SS (or other ligands, as specified) was added in conditions when specified. A control plasmid, pET-Luc2, was also tested in the presence and absence of 11 μM amino-*t*SS. All luminescence data were acquired using an ANDOR camera (EMCCD) at 25 °C and analyzed using Solis software, and images were further processed and analyzed using ImageJ.

To test whether Were-1 could regulate luciferase protein expression, samples were prepared under identical conditions and luminescence was measured for approximately 40 mins. Samples were then excited at 342 nm (Φ_q = 1.4*10^{-2} W/cm^2) for 1 s, and luminescence was recorded for approximately 30 mins. Samples were excited at 390 nm (Φ_q = 5.5*10^{-2} W/cm^2) for 1 s to switch Were-1 back to the bound 'off' state, and again, luminescence was measured for approximately 30 mins.

IC_{50} measurements. A dose-response of the Were-1 riboswitch to amino-*t*SS was assessed by measuring luminescence as a function of increasing target concentration. All data were acquired using an ANDOR camera and analyzed with Solis software, and images were further processed and analyzed using ImageJ, as described above.

***In vivo* translation kinetics.** Were-1-Fluc was transformed into BL21(DE3) *E. coli* cells and grown overnight in Luria Broth containing ampicillin (OD_{600} = 0.26). 1 mM IPTG was added to each well (containing 45 µL culture) to induce T7 RNA polymerase-driven expression and 100 µM D-luciferin to provide a substrate for Fluc. Amino-*t*SS or amino-*c*SS was also added where specified. Bioluminescence was recorded every five mins for one hour at 37 °C using a BioTek Synergy H1 plate reader.

To test whether the Were-1 riboswitch regulates the production of Fluc, samples were prepared under the same conditions. In the presence of amino-*t*SS, bioluminescence was measured on a BioTek Synergy H1 plate reader for approximately 15 mins before samples were excited at 342 nm for 1s in order to isomerize amino-*t*SS to amino-*c*SS.

Luminescence was recorded again for approximately 20 mins. Similar experiments were used regarding amino-*c*SS, with the exception of using 390 nm exposure for 0.5 ms in order to isomerize amino-*c*SS to amino-*t*SS, unless further specified.

***In vivo* light exposure analysis.** To determine the dependence of the amino-*t*SS exposure on the Were-1-Fluc expression, samples were prepared as described above and loaded into two black-bottom 96-well plates. One plate was used as a control and the other was exposed to 342 nm light ($\Phi_q = 1.4*10^{-2}$ W/cm^2) for their specified time using a Nikon FM-10 camera shutter in order to isomerize amino-*t*SS to amino-*c*SS. The same procedure was performed in the presence of amino-*c*SS, except 390 nm light was used ($\Phi_q = 5.5*10^{-2}$ W/cm^2) for their specified time to isomerize amino-*c*SS to amino-*t*SS. Bioluminescence was measured on an IVIS Lumina II imaging system 1 hr after light exposure.

To test whether the Were-1 riboswitch regulates the production of Fluc multiple times, samples were prepared as described above and loaded in a black-bottom 96-well plate. The top half of the plate was used as a control, containing the unresponsive G69C mutant, and the bottom half contained Were-1. All samples contained 10 μM amino-*t*SS and had their bioluminescence was measured 25 minutes after induction on a BioTek Synergy H1 plate reader. Next, the first group of wells remained unexposed to light and the middle and far right samples were exposed to 342 nm ($\Phi_q = 1.4*10^{-2}$ W/cm^2) for 1 ms. Measurements for all samples were taken 40 minutes after 342 nm exposure. Finally, the last group of wells (far right) were excited at 390 nm for 0.5 ms. Bioluminescence was

measured again, for all samples, 40 minutes after exposure. The same experiment was repeated with the inactive mutant, G69C, as an additional control. Data were normalized to the unexposed samples, and OD_{600} values were obtained to confirm that there was no cell death from UV damage.

IC_{50} measurements. A dose-response of the Were-1 riboswitch to the target metabolite (amino-*t*SS) was assessed by measuring bioluminescence inhibition as a function of increasing target concentration in BL21(DE3) *E. coli* cells. Bioluminescence was recorded under continuous conditions at 37 °C.

Data Availability: The authors declare that all data are available in the manuscript or the supplementary materials.

Acknowledgments

We thank the researchers who provided support for this study: Dalen Chan for synthesizing NAI, and Jennifer Prescher's lab for their luminescence reagents and IVIS setup. This work was supported by grants from the National Science Foundation (1804220 to A.L.), the National Institutes of Health (5T32GM108561-04 to K.A. R. and 5R01GM094929 to A.L.), the John Templeton Foundation (through the Foundation for Applied Molecular Evolution to A.L.), and the Czech Science Foundation (GACR 17-25897Y to J.M.).

2.6 Supplementary Information

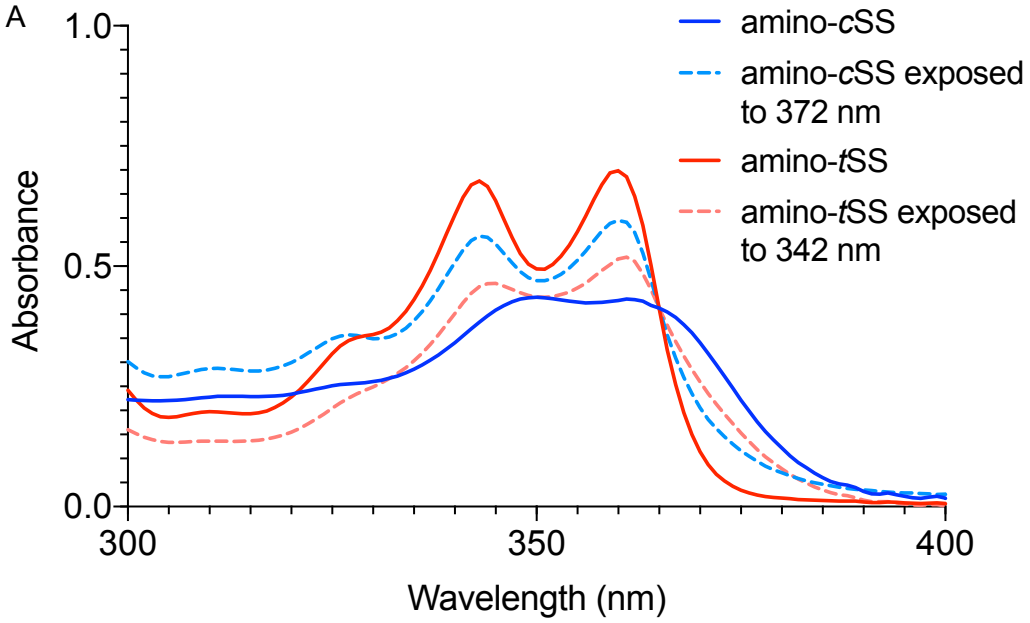

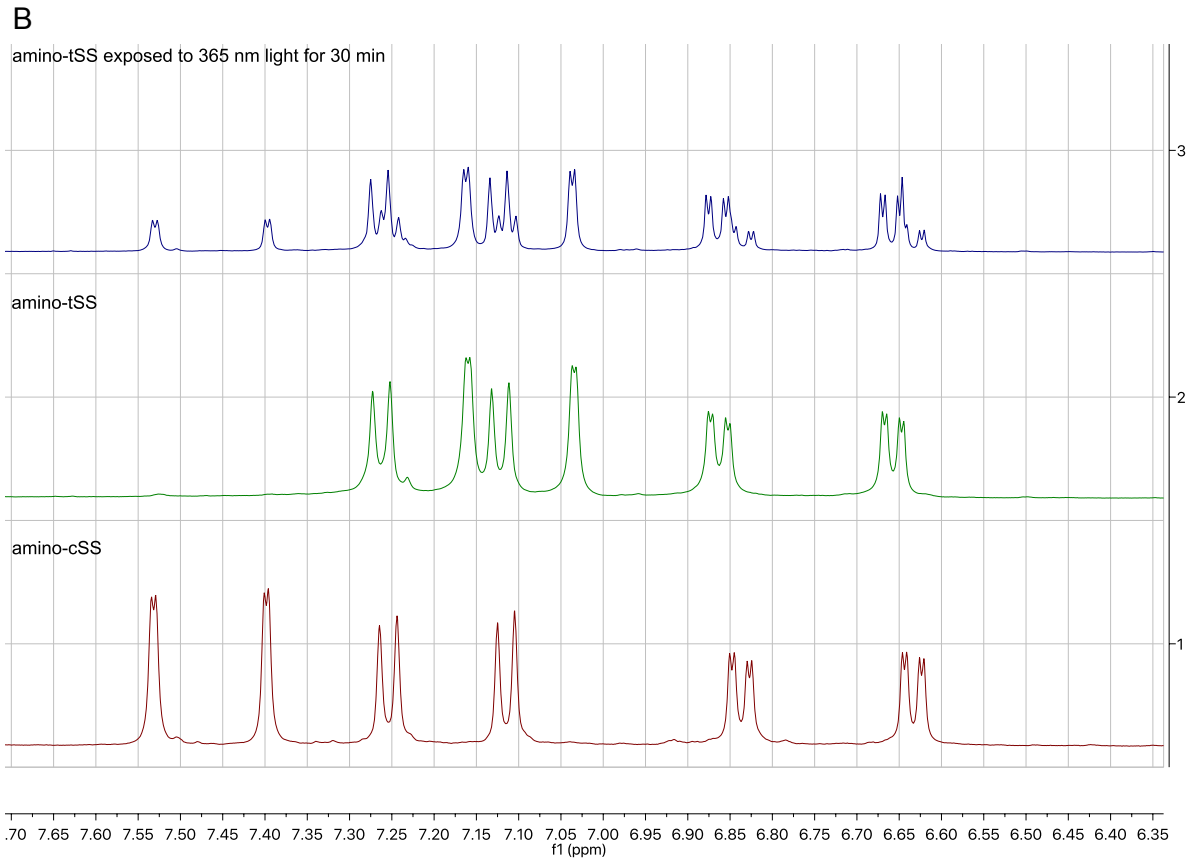

C

^{1}H NMR, *t*SS

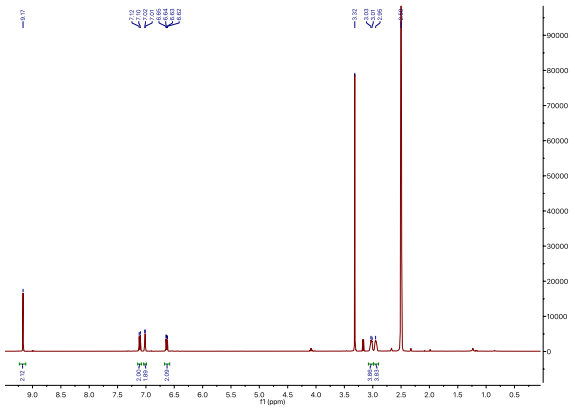

^{13}C NMR, *t*SS

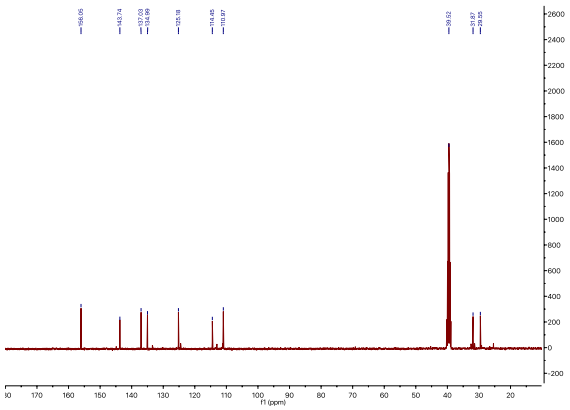

^{1}H NMR, amino-*t*SS

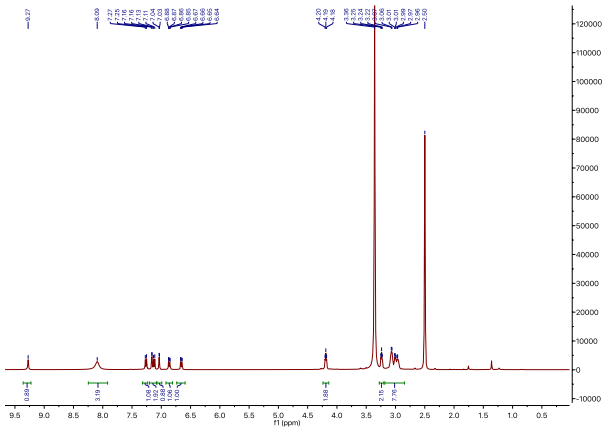

^{13}C NMR, amino-*t*SS

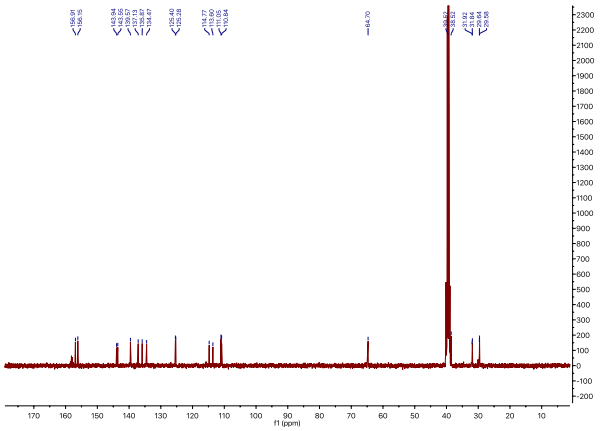

^{1}H NMR, amino-*c*SS

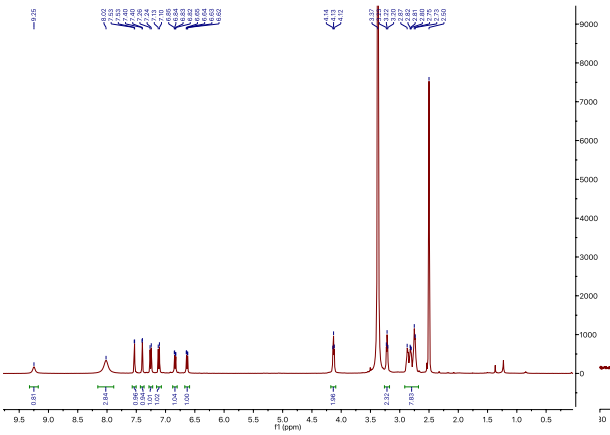

^{13}C NMR, amino-*c*SS

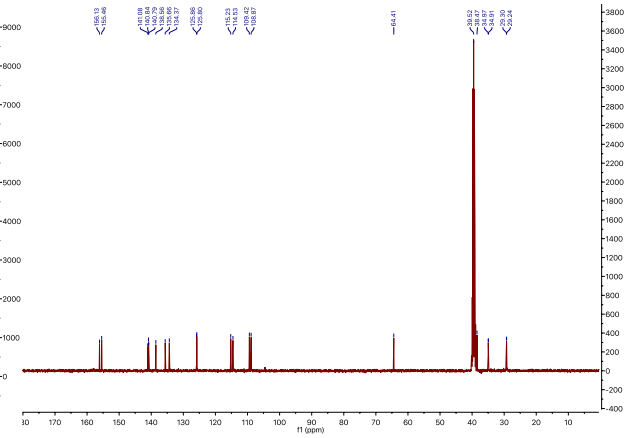

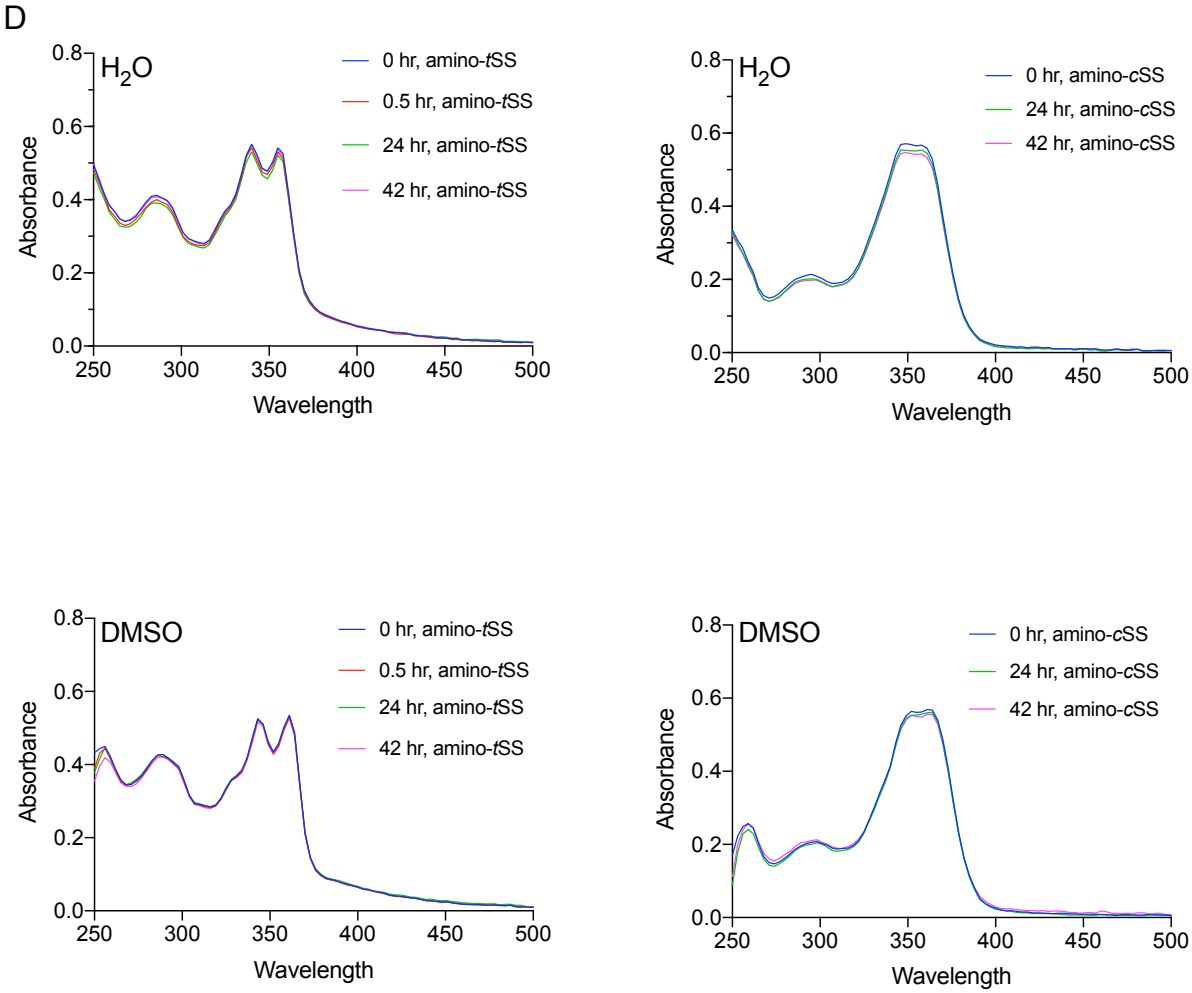

Supplementary Figure 2.1 | E/Z isomerization of amino-*t*SS and amino-*c*SS. a, UV-Vis spectra of amino-*t*SS (red) and amino-*t*SS after 3 h exposure to 342 nm (red, dashed), and amino-*c*SS (blue) and amino-*c*SS after 1.5 h exposure to 372 nm (blue, dashed). Photo isomerization was performed in 30 mM DMSO solutions and subsequently diluted 1000 times for UV-Vis spectra measurement. **b**, ^{1}H NMR of amino-*t*SS, amino-*c*SS, and E/Z isomerization. At the photostationary state (amino-*t*SS exposed to 365 nm) the ratio of amino-*t*SS to amino-*c*SS is approximately 2:1 as determined by NMR. **c**, ^{1}H NMR and ^{13}C NMR spectra of *t*SS (top), amino-*t*SS (middle), and amino-*c*SS (bottom). **d,** UV-Vis

spectra of amino-*t*SS and amino-*c*SS in H_2O (top) and DMSO (bottom). Both isoforms of the ligand are relatively stable in either solvent for the indicated times.

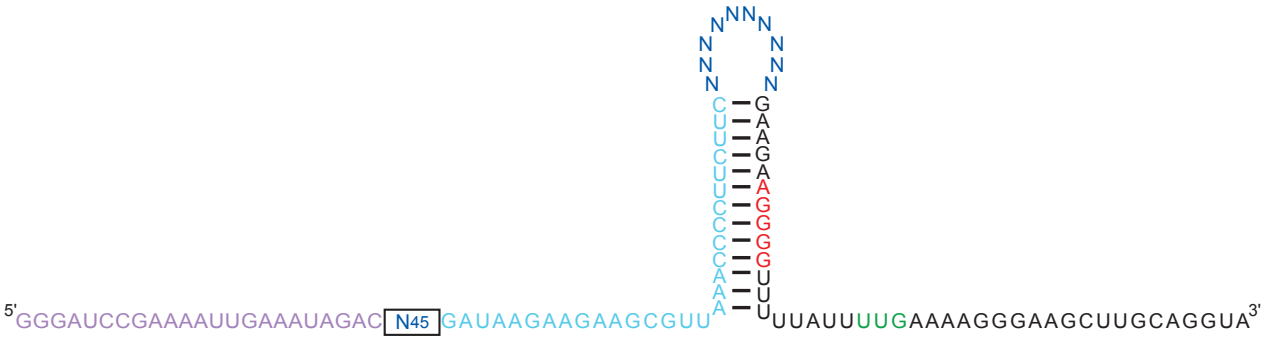

Supplementary Figure 2.2 | *In vitro* selection pool design for a photoriboswitch. An RNA pool was derived from *B. subtilis mswA* SAM-I riboswitch by replacing its ligand-binding domain with a 45-nucleotide random sequence (dark blue, boxed), partially randomizing (at a 15% level) its anti-terminator hairpin and the 5' half of the terminator hairpin (light blue), replacing the terminator-helix tetraloop sequence (UUAU) with a random decamer (dark blue), and retaining the 3' half of the terminator hairpin and its translation initiation sequences (red – Shine-Dalgarno; green – start codon). The pool's forward primer sequence (in RNA form) is shown in purple.

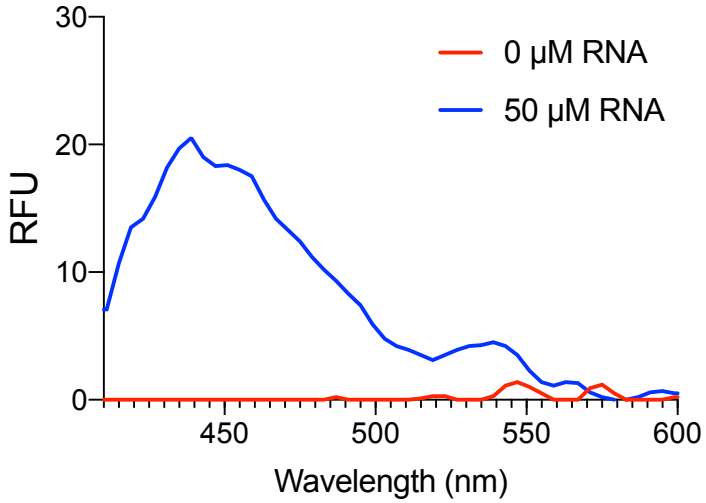

Supplementary Figure 2.3 | Screening of Were-1 based on optical activity. Fluorescence emission of 100 nM amino-*t*SS incubated with purified Were-1 RNA showing an increase in presence of Were-1 and suggesting RNA affinity for the target ligand. Emission spectra were collected using an excitation of 365/10 nm.

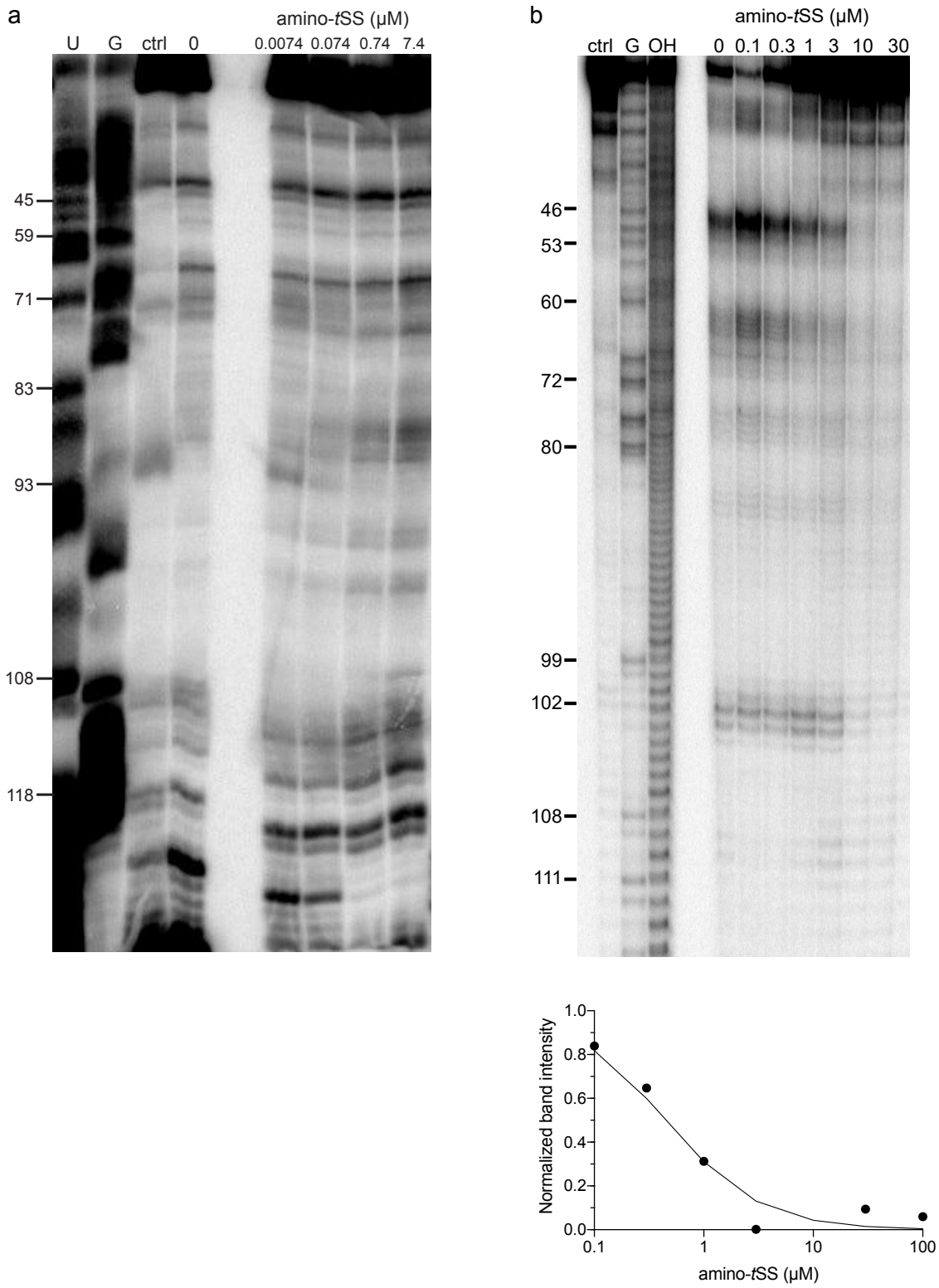
a
amino-tSS (μM)
U G ctrl 0 0.0074 0.074 0.74 7.4
45
59
71
83
93
108
118
b
amino-tSS (μM)
ctrl G OH 0 0.1 0.3 1 3 10 30
46
53
60
72
80
99
102
108
111
Normalized band intensity
1.0
0.8
0.6
0.4
0.2
0.0
0.1
1
10
100
amino-tSS (μM)

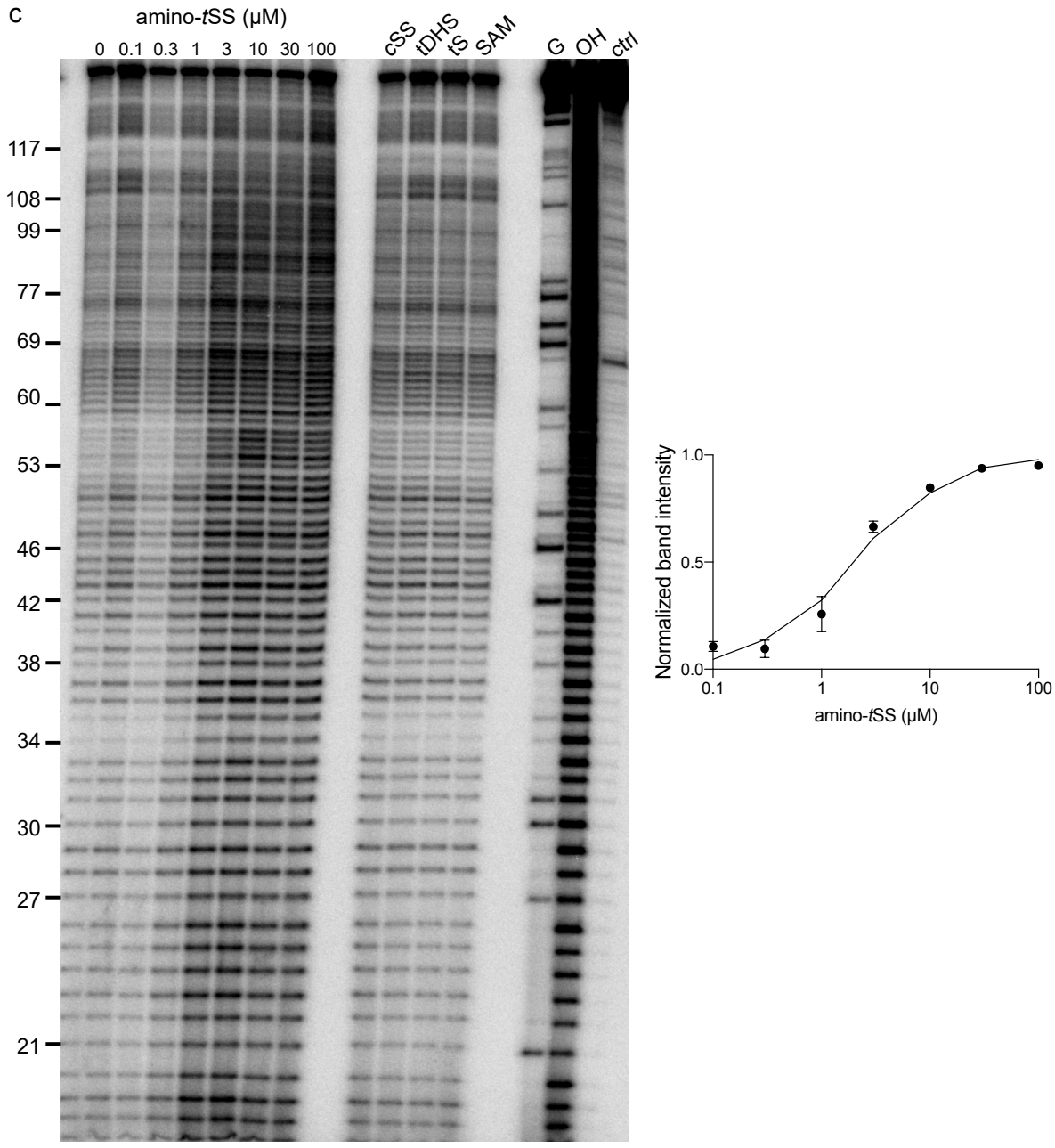
c
amino-tSS (μM)
0 0.1 0.3 1 3 10 30 100
cSS
tDHS
tS
SAM
G
OH
ctrl
117
108
99
77
69
60
53
46
42
38
34
30
27
21
Normalized band intensity
1.0
0.5
0.0
0.1
1
10
100
amino-tSS (μM)

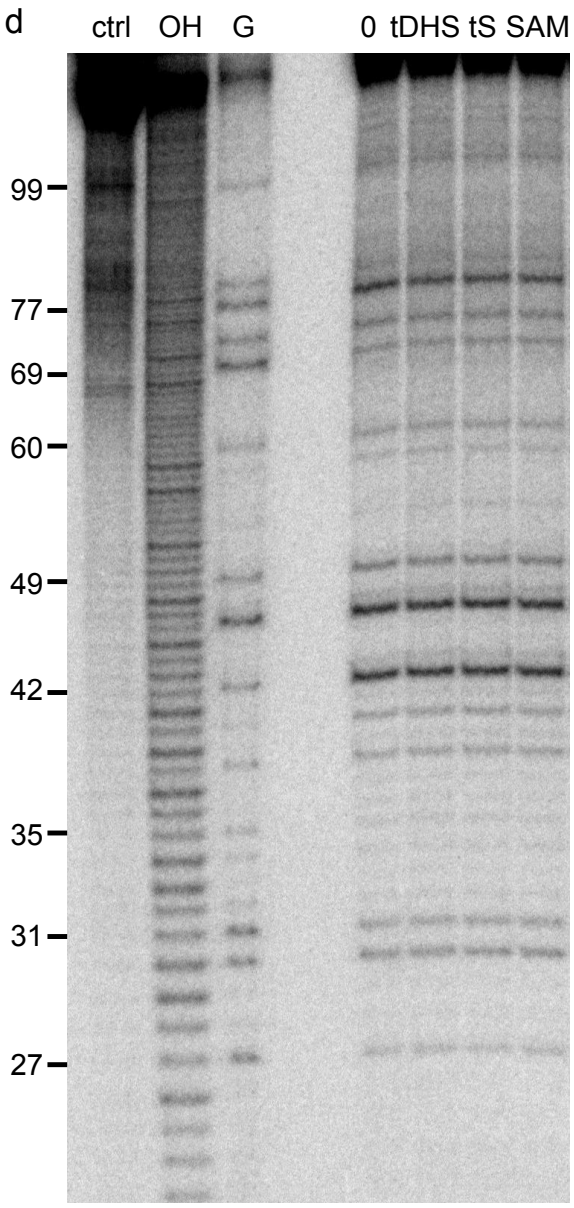
d
ctrl
OH
G
0
tDHS
tS
SAM
99
77
69
60
49
42
35
31
27

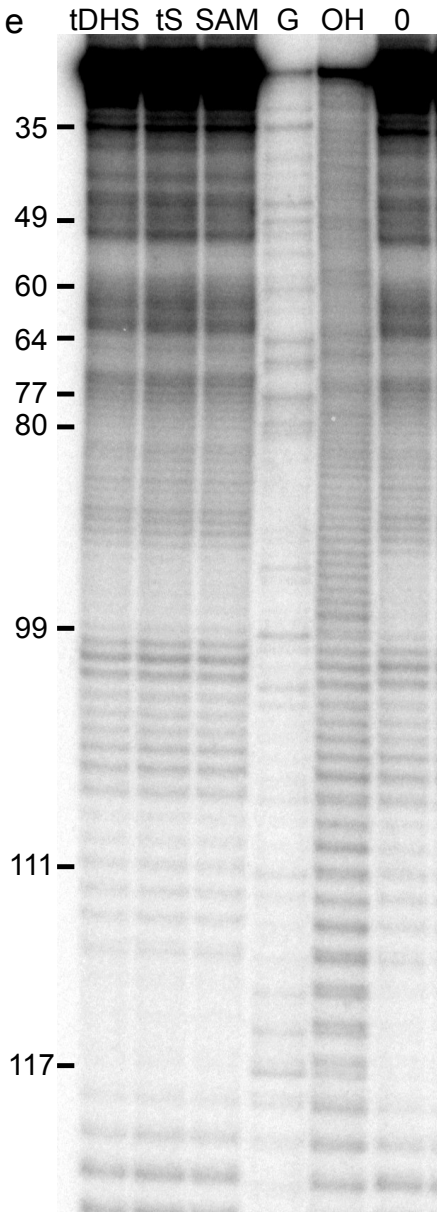
e
tDHS
tS
SAM
G
OH
0
35
49
60
64
77
80
99
111
117

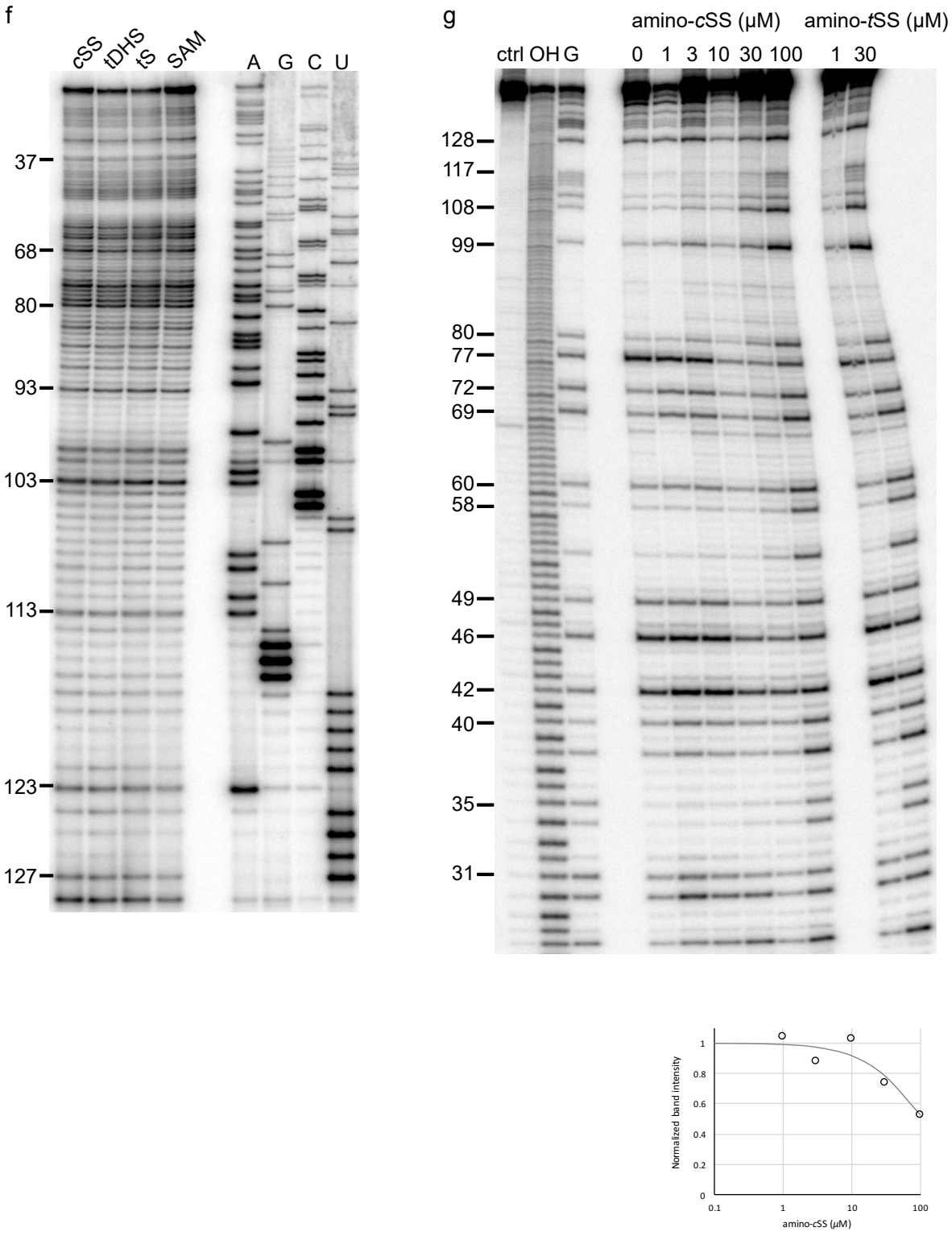
f
cSS
tDHS
tS
SAM
A G C U
37
68
80
93
103
113
123
127
g
amino-cSS (μM)
amino-tSS (μM)
ctrl OH G
0 1 3 10 30 100
1 30
128
117
108
99
80
77
72
69
60
58
49
46
42
40
35
31
Normalized band intensity
1
0.8
0.6
0.4
0.2
0
0.1
1
10
100
amino-cSS (μM)

Supplementary Figure 4 | **Structural probing of Werewolf-1. a**, SHAPE analysis of Were-1. Left lanes show reverse transcriptase (RT) stops due to ddA ("U") and ddC ("G") incorporation for sequence reference, followed by a no-acylation RT control (ctrl) lane, and SHAPE reactions with amino-*t*SS at concentrations indicated above the gel image. **b,** S1 digestion of Were-1. Left lanes contain a control with no RNA (ctrl), RNase T1 digestion for sequence reference, and a partial hydrolysis lane (OH). The right lanes show S1 digestion in the presence of increasing amino-*t*SS at concentrations indicated above the gel image. Analysis of the band intensity change at positions A44-G46 revealed an apparent K_D value of 0.4 μM (below). **c,** Terbium (III) footprinting of Were-1 in the presence of increasing amino-*t*SS. Left lanes show RNase T1 digestion for sequence reference, and partial hydrolysis (OH). Middle lanes show Tb^{3+} footprinting in the presence of increasing amino-*t*SS at concentrations indicated above the gel image. Right lanes show control reactions with Were-1 in the presence of 30 μM controls, as labeled above the gel image. Right, a K_D value of 4.8 μM was calculated based on the change in intensity with increasing amino-*t*SS at nucleotides A113 and U107. **d,** T1 digestion controls. Left lanes contain a control with no RNA, partial hydrolysis (OH), and RNase T1 digestion for sequence reference. Right lanes indicate no ligand (0), followed by Were-1 in the presence of 30 μM controls, as labeled above the gel image. **e,** In-line probing of Were-1 with 30 μM controls, as labeled above the gel image, followed by RNase T1 digestion for sequence reference, partial hydrolysis (OH), and a no ligand control (0). **f,** SHAPE of Were-1 in presence of control small molecules. Left lanes show RT stops for Were-1 in the presence of 30 μM amino-*c*SS, tDHS, tS, and SAM. Right lanes show RT stops due to ddT ("A"), ddC ("G"), ddG ("C"), and ddA ("U") incorporation for sequence

reference. **g,** T1 digestion of Were-1 in the presence of increasing amino-*c*SS. Left lanes show undigested RNA, partial hydrolysis, and a G-specific sequencing lane. Middle lanes show Were-1 digestion in the presence of increasing amino-*c*SS and the right lane show amino-*t*SS experiments at low and high concentrations, for direct comparison of the ligand-induced structural probing. At high concentration (100 μM) amino-*c*SS mimics the bound profile of amino-*t*SS. The apparent K_D calculation for *c*SS is shown below the gel image and in Fig. 1b, revealing a K_D of 108 μM.

A

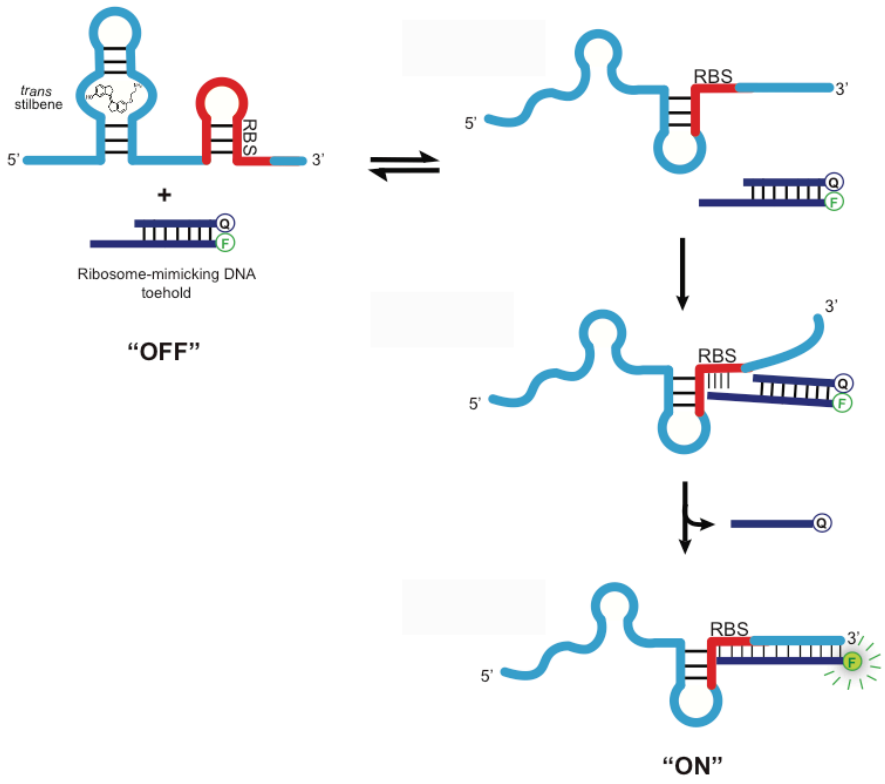
trans
stilbene
RBS
5'
3'
+
Ribosome-mimicking DNA
toehold
"OFF"
RBS
5'
3'
Q
F
"ON"

B

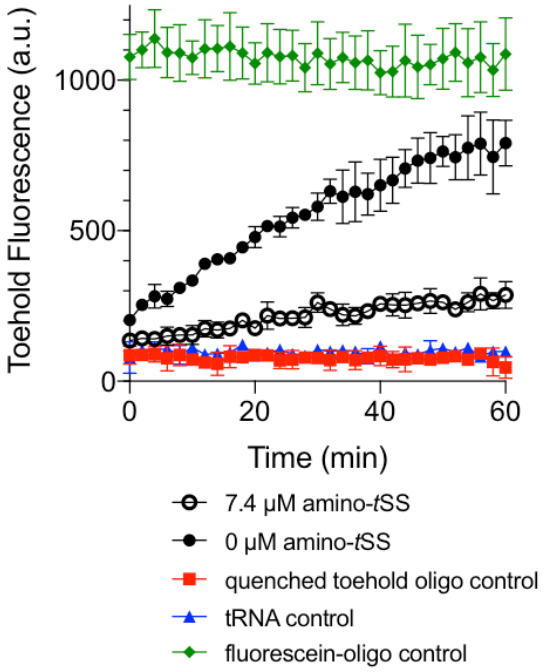
Toehold Fluorescence (a.u.)
1000
500
0
0
20
40
60
Time (min)
7.4 μM amino-tSS
0 μM amino-tSS
quenched toehold oligo control
tRNA control
fluorescein-oligo control

C

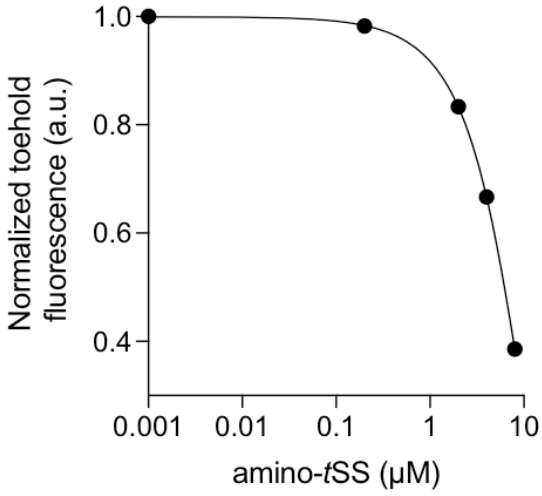
Normalized toehold
fluorescence (a.u.)
1.0
0.8
0.6
0.4
0.001
0.01
0.1
1
10
amino-tSS (μM)

Supplementary Figure 2.5 | Binding PAGE-purified Were-1 RNA to a ribosome-mimic. a, Schematic of strand displacement, where a DNA duplex containing a toehold complementary to the Shine-Dalgarno sequence of Were-1 is displaced when no amino-*t*SS is present, producing a fluorescence. **b**, The presence of amino-*t*SS prevents the quencher strand release, suppressing toehold fluorescence (± SD) over time. Control reactions were performed using the unquenched fluorophore oligo (green) and the quenched toehold oligo (red) for fully quenched fluorescence to provide a window for maximum fluorescence, and a tRNA (blue) lacking the Shine-Dalgarno sequence as a negative control. **c**, Dose-response curve of PAGE-purified Were-1 RNA in the presence of increasing concentrations of amino-*t*SS and analyzed by the toehold-fluorescence assay. Half maximum fluorescence is observed at 6.3 μM amino-*t*SS.

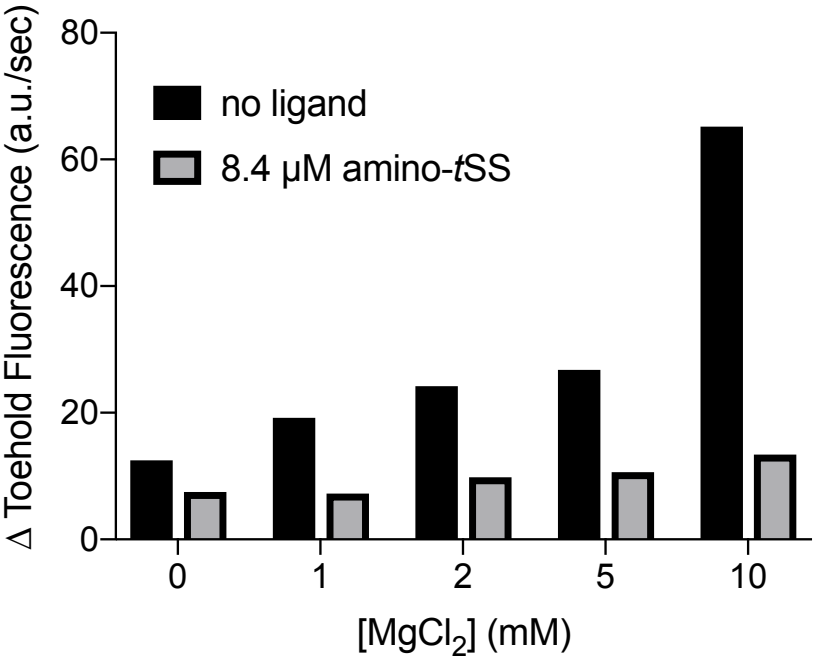

Supplementary Figure 2.6 | Co-transcriptional binding of a ribosome-mimic *in vitro* under various Mg^{2+} conditions. Whereas the rate of transcription increases with magnesium (black), the bound state (gray) does not change significantly, suggesting that co-transcriptional binding is minimally affected by magnesium concentration.

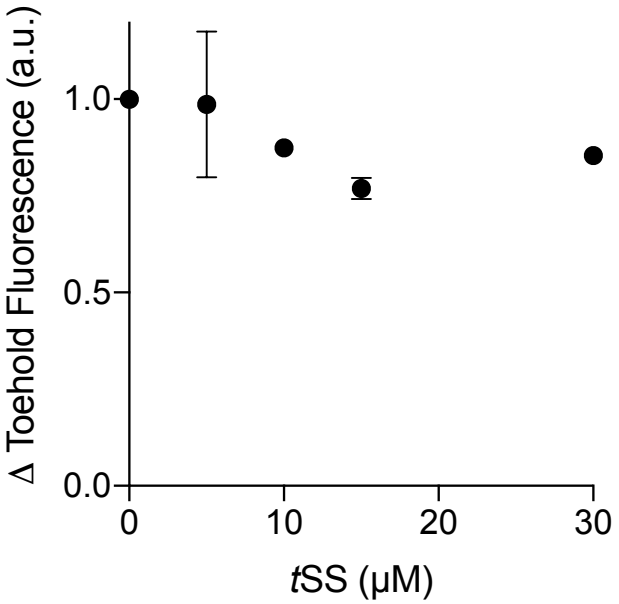

Supplementary Figure 2.7 | Co-transcriptional Were-1 binding of a ribosome-mimic *in vitro* in the presence of *t*SS (in 10 % DMSO). A minor dose-response is observed in the presence of increasing *t*SS concentrations, but full inhibition, as seen for amino-*t*SS, is not observed, possibly due to low solubility of *t*SS.

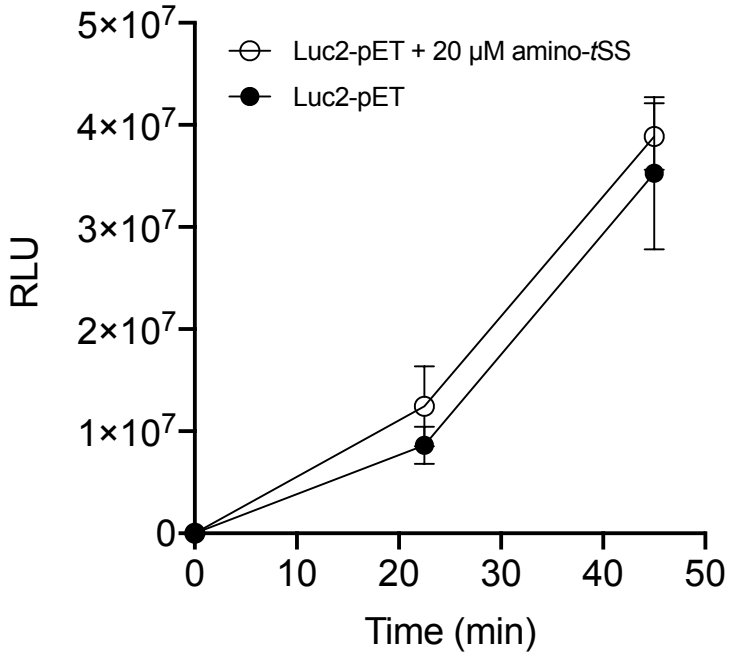

Supplementary Figure 2.8 | Translation of a control plasmid, Luc2-pET, lacking the Were-1 riboswitch is not inhibited *in vitro* by amino-*t*SS. There is no significant difference in Luc2-pET luminescence (± SD) in the presence and absence of amino-*t*SS, suggesting that amino-*t*SS does not inhibit the *in vitro* translation system.

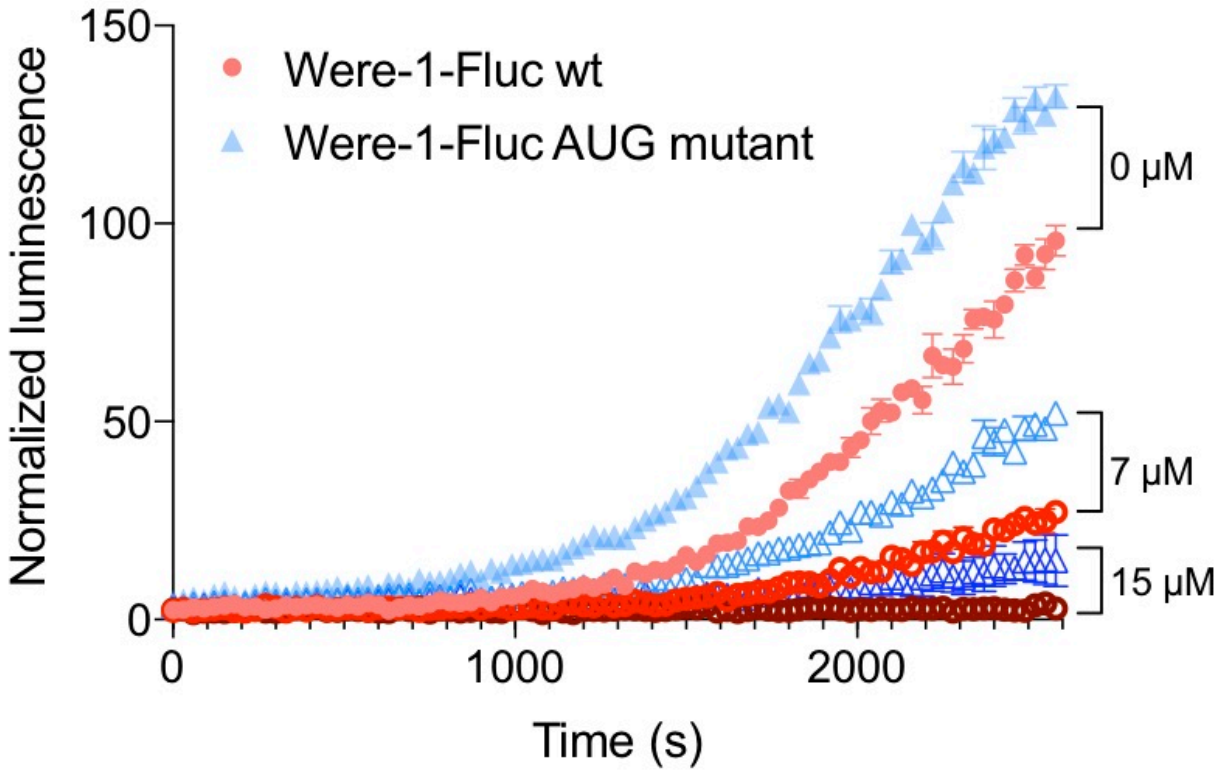

Supplementary Figure 2.9 | The effect of the canonical start codon on Were-1-Fluc expression *in vivo*. Comparison of luciferase expression (± SEM) of Were-1-Fluc wild-type (wt; red) and Were-1-Fluc containing an AUG start codon (Were-1-Fluc AUG mutant; blue), in place of the pool-derived UUG minor start codon, with increasing amino-*t*SS concentrations. Bioluminescence was overall higher in the Were-1-Fluc AUG mutants for all conditions but retained the wt dose-dependent response.

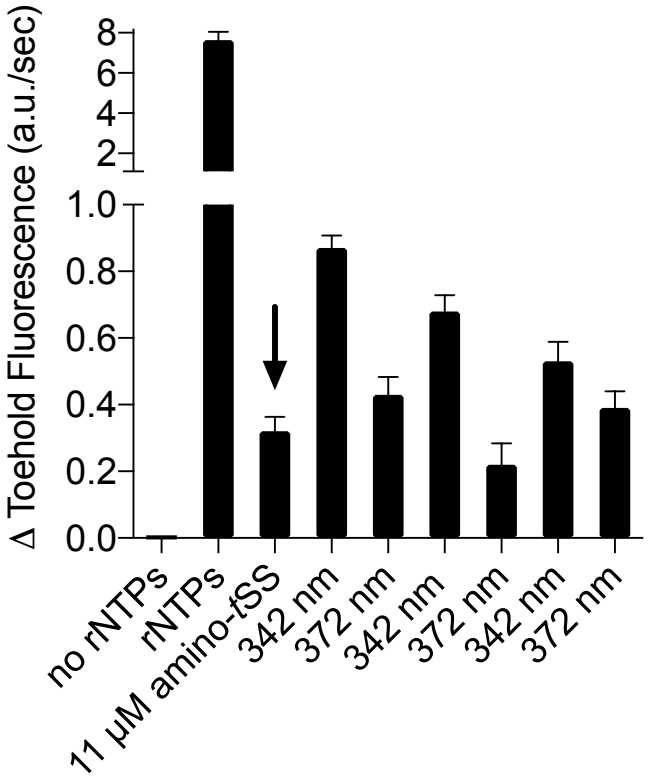

Supplementary Figure 2.10 | Co-transcriptional binding of a ribosome-mimic *in vitro* under amino-*t*SS photoisomerization conditions. Initial transcription of Were-1 without ligand was induced by adding ribonucleoside triphosphates (rNTPs) to a transcription mix, producing robust toehold fluorescence increase (see Fig. 2b for examples of co-transcriptional toehold binding). Upon adding 11 μM amino-*t*SS (arrow), fluorescence growth decreased, suggesting that Were-1 is bound to the ligand and prevents toehold binding. The sample was then exposed to 342 nm ($\Phi_q = 6.8*10^{-5}$ W/cm^2) for 60 s, causing photoisomerization of the ligand, and resulting in increased toehold fluorescence slope. Were-1 transcription reaction was subsequently exposed to 372 nm

light (Φ_q = 1*10^{-4} W/cm^2) for 60 s, to switch the ligand from *cis* to *trans* conformation, which resulted in decrease of toehold fluorescence slope. This was repeated two more times, as indicated, until the transcription reaction plateaued, and all toehold was expended. The data suggest that the system can be regulated multiple times in one reaction. Error bars represent fluorescence slope error.

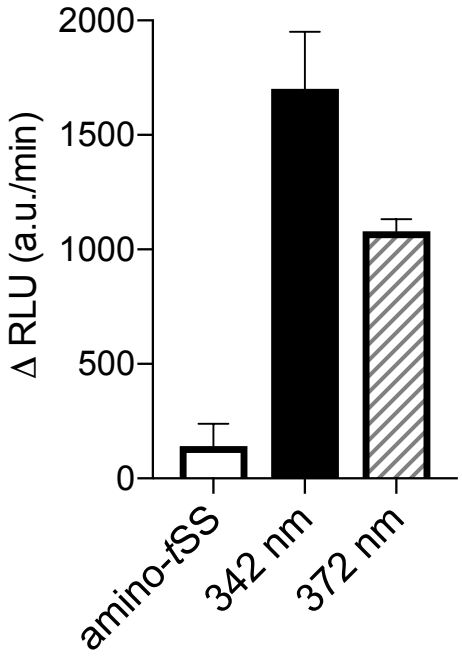

Supplementary Figure 2.11 | **Were-1 regulates translation *in vitro*.** *In vitro* transcription-translation reaction of Were-1-Fluc mRNA in presence of amino-*t*SS (left column) was irradiated at 342 nm for 60 s, resulting in an increase in luciferase production (± SEM). The reaction was then irradiated at 372 nm for 60 s, resulting in a decrease in luciferase expression rate (± SEM) over time.

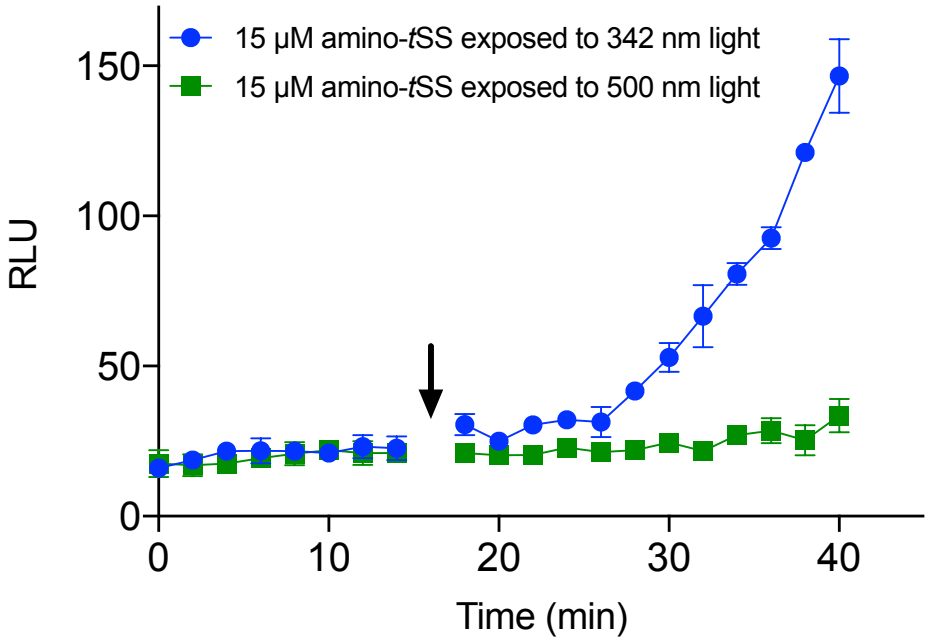

Supplementary Figure 2.12 | **Were-1 regulates protein expression *in vivo.*** Were-1 *E. coli* bioluminescence (± SEM) was measured in the presence of amino-*t*SS. Initial Fluc expression showed identical increases in bioluminescence for all samples. In the presence of 15 *μ*M amino-*t*SS, samples were either exposed to (arrow) 342 nm light (blue) to isomerize amino-*t*SS, or 500 nm (green), a wavelength that does not affect amino-*t*SS isomerization. 342-nm–exposed samples showed significantly higher bioluminescence compared to those exposed to 500 nm light.

Supplementary Table 2.1 | DNA sequences used for *in vitro* and *in vivo* analysis of the Were-1 riboswitch.

Toehold-Fluorophore Reporter	Rep F: 5'– 5FluorT/TA CCTGCAAGCTTCCCTTTTCAAAATAAAAACCCCT –3' Rep Q: 5'– ATTTTGAAAAGGGAAGCTTGCAGGTA/3IABkFQ –3'
Forward Overhang Primer (AL2909)	5'– CCCgaattcTAATACGACTCACTATAGGGATCCGAAAATTGAAATAGAC –3'
Reverse Overhang Primer (AL2912)	5'– atggcgccgggcctttctttatgtttttggcgtcttCCCTGCAAGCTTCCCTTTTCAAAATAAAAAC –3'
Forward Werewolf Primer (AL2881)	5'– GGGATCCGAAAATTGAAATAGACTCC –3'
Reverse Nested Fluc Primer (AL1649)	5'– gattctgtgatttgtattcagcccata –3'
Pool Forward Primer (AL2045)	5'– TAATACGACTCACTATAGGGATCCGAAAATTGAAATAGAC –3'
Pool Reverse Primer (AL2049)	5'– TACCTGCAAGCTTCCCTTTTC –3'
AUG mutant Forward Primer (AL3267)	5'– 5Phos/ATGAAAAGGGAAGCTTGCAGGgaagac –3'
AUG mutant Reverse Primer (AL3268)	5'– /5Phos/AA TAA AAA CCC CTT CTT CAA GGT TGG CTG AAG –3'
C89G mutant Forward Primer (AL3330)	5'– /5Phos/GACATCTTCAGCCAACCTTG – 3’
C89G mutant Reverse Primer (AL3331)	5'– /5Phos/GTTTGATGCTTCTGGTCATCTG –3'
G69C mutant Forward Primer (AL3328)	5'– /5Phos/CATGACCAGAAGCATCAAACCAC –3'

G69C mutant Reverse Primer (AL3329)	5'– /5Phos/TGGTAATTCACGGTGCTTACTGC –3'
C91G mutant Forward Primer (AL3326)	5'– /5Phos/GATCTTCAGCCAACCTTGAAGAAGG –3'
C91G mutant Reverse Primer (AL3327)	5'– /5Phos/TGGTTTGATGCTTCTGGTCATCTG –3'
C84G/G69C compensatory mutant Forward Primer (AL3384)	5'– /5Phos/GAAACCACATCTTCAGCCAACCTT–3'
C84G/G69C compensatory mutant Reverse Primer (AL3385)	5'– /5Phos/ATGCTTCTGGTCATGTGGTAATTCAC –3'
Were-1 DNA	5'– GGGATCCGAAAATTGAAATAGACTCCGATGGACGGTTGCGTGTATGCAGTAAGCACCGTGAATTACCAGATGACCAGAAGCATCAAACCACATCTTCAGCCAACCTTGAAGAAGGGGTTTTTATTTTGAAAAGGGAAGCTTGCAGGTA –3'
Amino-*t*SS pool	5'– TAATACGACTCACTATAGGGATCCGAAAATTGAAATAGAC11111111111111111111111111111111111111111111111111145255455455434225553333223223111111111GAAGAAGGGGTTTTTATTTTGAAAAGGGAAGCTTGCAGGTA–3'
Were-1-Fluc construct	5'– TAATACGACTCACTATAGGGATCCGAAAATTGAAATAGACTCCGATGGACGGTTG

	CGTGTATGCAGTAAGCACCGTGAATTACCAGATGACCAGAAGCATCAAACCACAT CTTCAGCCAACCTTGAAGAAGGGGTTTTTATTTTGAAAAGGGAAGCTTGCAGGgaag acgccaaaaacataaagaaaggcccggcgccattctatccgctggaagatggaaccgctggagagcaactgcataaggctatgaaga gatacgccctggttcctggaacaattgcttttacagatgcacatatcgaggtggacatcacttacgctgagtacttcgaaatgtccgttcggt tggcagaagctatgaaacgatatgggctgaatacaaatcacagaatcgtcgtatgcagtgaaaactctcttcaattctttatgccggtgttg ggcgcgttatttatcggagttgcagttgcgcccgcgaacgacatttataatgaacgtgaattgctcaacagtatgggcatttcgcagcctac cgtggtgttcgtttccaaaaaggggttgcaaaaaattttgaacgtgcaaaaaaagctcccaatcatccaaaaaattattatcatggattctaa aacggattaccagggatttcagtcgatgtacacgttcgtcacatctcatctacctcccggttttaatgaatacgattttgtgccagagtccttc gatagggacaagacaattgcactgatcatgaactcctctggatctactggtctgcctaaaggtgtcgctctgcctcatagaactgcctgcg tgagattctcgcatgccagagatcctatttttggcaatcaaatcattccggatactgcgattttaagtgttgttccattccatcacggttttggaa tgtttactacactcggatatttgatatgtggatttcgagtcgtcttaatgtatagatttgaagaagagctgtttctgaggagccttcaggattac aagattcaaagtgcgctgctggtgccaaccctattctccttcttcgccaaaagcactctgattgacaaatacgatttatctaatttacacgaaa ttgcttctggtggcgctcccctctctaaggaagtcggggaagcggttgccaagaggttccatctgccaggtatcaggcaaggatatggg ctcactgagactacatcagctattctgattacacccgaggggatgataaaccgggcgcggtcggtaaagttgttccatttttgaagcga aggttgtggatctggataccgggaaaacgctgggcgttaatcaaagaggcgaactgtgtgtgagaggtcctatgattatgtccggttatgt aaacaatccggaagcgaccaacgccttgattgacaaggatggatggctacattctggagacatagcttactgggacgaagacgaacac ttcttcatcgttgaccgcctgaagtctctgattaagtacaaaggctatcaggtggctcccgctgaattggaatccatcttgctccaacacccc aacatcttcgacgcaggtgtcgcaggtcttcccgacgatgacgccggtgaacttcccgccgccgttgttgttttggagcacggaaagac gatgacggaaaaagagatcgtggattacgtcgccagtcaagtaacaaccgcgaaaaagttgcgcggaggagttgtgtttgtggacgaa gtaccgaaaggtcttaccggaaaactcgacgcaagaaaaatcagagagatcctcataaaggccaagaagggcggaaagatcgccgt gtaa–3'

Abbreviations/Key

3IABkFQ – 3' Iowa black fluorophore quencher

5FluorT – 5' Fluorescein

1 A:G:C:T=1:1:1:1

2 A:G:C:T=17:1:1:1

3 A:G:C:T=1:17:1:1

4 A:G:C:T=1:1:17:1

5 A:G:C:T=1:1:1:17

2.7 References

1. Fenno, L., Yizhar, O. & Deisseroth, K. The Development and Application of Optogenetics. *Annu. Rev. Neurosci.* **34,** 389–412 (2011).
2. Möglich, A. & Moffat, K. Engineered photoreceptors as novel optogenetic tools. *Photochem. Photobiol. Sci.* **9,** 1286 (2010).
3. Motta-Mena, L. B. *et al.* An optogenetic gene expression system with rapid activation and deactivation kinetics. *Nat. Chem. Biol.* **10,** 196–202 (2014).
4. Cambridge, S. B. *et al.* Doxycycline-dependent photoactivated gene expression in eukaryotic systems. *Nat. Methods* **6,** 527–531 (2009).
5. Dhamodharan, V., Nomura, Y., Dwidar, M. & Yokobayashi, Y. Optochemical control of gene expression by photocaged guanine and riboswitches. *Chem. Commun.* **54,** 6181–6183 (2018).
6. Wulffen, B., Buff, M. C. R., Pofahl, M., Mayer, G. & Heckel, A. Caged glucosamine-6-phosphate for the light-control of riboswitch activity. *Photochem. Photobiol. Sci.* **11,** 489–492 (2012).
7. Walsh, S., Gardner, L., Deiters, A. & Williams, G. J. Intracellular Light-Activation of Riboswitch Activity. *ChemBioChem* **15,** 1346–1351 (2014).
8. Young, D. D., Garner, R. A., Yoder, J. A. & Deiters, A. Light-activation of gene function in mammalian cells via ribozymes. *Chem. Commun. (Camb).* 568–70 (2009). doi:10.1039/b819375d
9. Chaulk, S. & MacMillan, A. M. Caged RNA: photo-control of a ribozyme reaction. *Nucleic Acids Res.* **26,** 3173–3178 (1998).
10. Lucas, T. *et al.* Light-inducible antimiR-92a as a therapeutic strategy to promote

skin repair in healing-impaired diabetic mice. *Nat. Commun.* **8,** 15162 (2017).

11. Lee, H.-W., Robinson, S. G., Bandyopadhyay, S., Mitchell, R. H. & Sen, D. Reversible Photo-regulation of a Hammerhead Ribozyme Using a Diffusible Effector. *J. Mol. Biol.* **371,** 1163–1173 (2007).
12. Hayashi, G., Hagihara, M. & Nakatani, K. RNA Aptamers That Reversibly Bind Photoresponsive Azobenzene-Containing Peptides. *Chem. - A Eur. J.* **15,** 424–432 (2009).
13. Lotz, T. S. *et al.* A light-responsive RNA aptamer for an azobenzene derivative. *Nucleic Acids Res.* (2018). doi:10.1093/nar/gky1225
14. Young, D. D. & Deiters, A. Light-Regulated RNA-Small Molecule Interactions. *ChemBioChem* **9,** 1225–1228 (2008).
15. Tuerk, C. & Gold, L. Systematic evolution of ligands by exponential enrichment: RNA ligands to bacteriophage T4 DNA polymerase. *Science* **249,** 505–10 (1990).
16. Ellington, A. D. & Szostak, J. W. In vitro selection of RNA molecules that bind specific ligands. *Nature* **346,** 818–822 (1990).
17. Martini, L. *et al. In Vitro* Selection for Small-Molecule-Triggered Strand Displacement and Riboswitch Activity. *ACS Synth. Biol.* **4,** 1144–1150 (2015).
18. Quick, M. *et al.* Photoisomerization Dynamics of Stiff-Stilbene in Solution. *J. Phys. Chem. B* **118,** 1389–1402 (2014).
19. Waldeck, D. H. Photoisomerization Dynamics of Stilbenes. *Chem. Rev* **91,** 415–436 (1991).
20. Szymanski, W., Beierle, J. M., Kistemaker, H. A. V, Velema, W. A. & Feringa, B. L. Reversible Photocontrol of Biological Systems by the Incorporation of

Molecular Photoswitches Wiktor Szyman sBeierle, J. M., Kistemaker, H. A. V, Velema, W. A., & Feringa, B. L. (2013). Reversible Photocontrol of Biological Systems by the Incorporation of. *Chem. Rev.* **113,** 6114–6178 (2013).

21. You, M. & Jaffrey, S. R. Designing optogenetically controlled RNA for regulating biological systems. *Ann. N. Y. Acad. Sci.* **1352,** 13–19 (2015).
22. Liang, J. C., Bloom, R. J. & Smolke, C. D. Engineering Biological Systems with Synthetic RNA Molecules. *Mol. Cell* **43,** 915–926 (2011).
23. Jäschke, A. Genetically encoded RNA photoswitches as tools for the control of gene expression. *FEBS Lett.* **586,** 2106–2111 (2012).
24. Mondal, P., Granucci, G., Rastädter, D., Persico, M. & Burghardt, I. Azobenzene as a photoregulator covalently attached to RNA: a quantum mechanics/molecular mechanics-surface hopping dynamics study. *Chem. Sci.* **9,** 4671–4681 (2018).
25. Brieke, C., Rohrbach, F., Gottschalk, A., Mayer, G. & Heckel, A. Light-Controlled Tools. *Angew. Chemie Int. Ed.* **51,** 8446–8476 (2012).
26. Akinwumi, B. *et al.* Biological Activities of Stilbenoids. *Int. J. Mol. Sci.* **19,** 792 (2018).
27. Sirerol, J. A. *et al.* Role of Natural Stilbenes in the Prevention of Cancer. *Oxid. Med. Cell. Longev.* **2016,** 1–15 (2016).
28. Tan, W., Zhou, J., Li, F., Yi, T. & Tian, H. Visible Light-Triggered Photoswitchable Diarylethene-Based Iridium(III) Complexes for Imaging Living Cells. *Chem. – An Asian J.* **6,** 1263–1268 (2011).
29. Stauch, T. & Dreuw, A. Stiff-stilbene photoswitch ruptures bonds not by pulling but by local heating. *Phys. Chem. Chem. Phys.* **18,** 15848–15853 (2016).

30. Deperasińska, I. *et al.* Low-Temperature Spectra of the Analogues of 10-Hydroxybenzo[*h*]quinoline as an Indication of Barrierless ESIPT. *J. Phys. Chem. A* **116,** 12049–12055 (2012).

31. Winkler, W. C., Nahvi, A., Sudarsan, N., Barrick, J. E. & Breaker, R. R. An mRNA structure that controls gene expression by binding S-adenosylmethionine. *Nat. Struct. Biol.* **10,** 701–707 (2003).

32. Peng, Y., Soper, T. J. & Woodson, S. A. RNase footprinting of protein binding sites on an mRNA target of small RNAs. *Methods Mol. Biol.* **905,** 213–24 (2012).

33. Reynolds, W. F. & Gottesfeld, J. M. Torsional stress induces an S1 nuclease-hypersensitive site within the promoter of the Xenopus laevis oocyte-type 5S RNA gene. *Proc. Natl. Acad. Sci. U. S. A.* **82,** 4018 (1985).

34. Harris, D. A., Todd, G. C. & Walter, N. G. in *Handbook of RNA Biochemistry* 255–268 (Wiley-VCH Verlag GmbH & Co. KGaA, 2014). doi:10.1002/9783527647064.ch12

35. Regulski, E. E. & Breaker, R. R. in 53–67 (Humana Press, 2008). doi:10.1007/978-1-59745-033-1_4

36. Wilkinson, K. A., Merino, E. J. & Weeks, K. M. Selective 2′-hydroxyl acylation analyzed by primer extension (SHAPE): quantitative RNA structure analysis at single nucleotide resolution. *Nat. Protoc.* **1,** 1610–1616 (2006).

37. Martini, L., Ellington, A. D. & Mansy, S. S. An in vitro selection for small molecule induced switching RNA molecules. *Methods* **106,** 51–57 (2016).

38. Zhang, D. Y. & Winfree, E. Control of DNA Strand Displacement Kinetics Using Toehold Exchange. *J. Am. Chem. Soc.* **131,** 17303–17314 (2009).

39. Frieda, K. L. & Block, S. M. Direct observation of cotranscriptional folding in an adenine riboswitch. *Science* **338,** 397–400 (2012).

40. Grundy, F. J. & Henkin, T. M. The S box regulon: a new global transcription termination control system for methionine and cysteine biosynthesis genes in gram-positive bacteria. *Mol. Microbiol.* **30,** 737–49 (1998).

41. Band, L. & Henner, D. J. Bacillus subtilis requires a 'stringent' Shine-Dalgarno region for gene expression. *DNA* **3,** 17–21 (1984).

42. Spitale, R. C. *et al.* RNA SHAPE analysis in living cells. *Nat. Chem. Biol.* **9,** 18–20 (2013).

43. Lorenz, R. *et al.* ViennaRNA Package 2.0. *Algorithms Mol. Biol.* **6,** 26 (2011).

Chapter 3: Co-transcriptional mRNA Activation and Inhibition of a Ribosome-mimic *In Vitro*

3.1 Introduction

One key principle in biology is that structure determines function[1]. During co-transcriptional folding, nascent RNAs have the potential to interact with ligands and form alternative structures[2]. For example, the rate of transcription directly impacts the window of when a ligand can bind to a riboswitch and influence its folded structure, before a termination decision is made[3].

There are at least two flavin mononucleotide (FMN) riboswitches in *B. subtilis*, one that controls translation initiation (*ypaA*) and one that controls transcription termination (*ribD*)[4]. The speed of RNA transcription was first studied in the *ribD* FMN riboswitch where the authors identified how the rate of transcription affected metabolite binding kinetics of the RNA to its metabolite, riboflavin, while RNA polymerase is paused[5]. This suggested that the FMN riboswitch was kinetically driven rather than thermodynamically driven. Other studies have shown that the rate of transcription is critical for co-transcriptional binding of adenine for the *B. subtilis pbuE* riboswitch to perform efficiently, whereas the translational riboswitch *V. vulnificus*, which also binds adenine, is able to bind its ligand after transcription and still fully function[6]. Additionally, these two adenine riboswitches have different mechanisms of gene regulation; beyond the obvious difference in transcription and translation control, the *V. vulnificus* riboswitch relies on reversible ligand binding[7].

In this study, we investigated two additional clones from our RNA pool[8] to determine whether we could expand our library of photoriboswitches as optogenetic tools. In two clones, Clone 29 and Clone 10, we identified that both RNAs are able to co-transcriptionally activate and inhibit a ribosomal-mimic upon binding a *trans* stiff stilbene (amino-*t*SS) *in vitro* depending upon the promoter and polymerase used. Based on the structure and co-transcriptional binding data for both sequences, it is possible that both RNAs can regulate transcription and translation, but these processes need to be investigated further. A brief look into each clone's structure and *in vitro* kinetics is summarized below, followed by the future directions needed to complete the analysis of this study.

3.2 Results and Discussion

To further develop the RNA optogenetic toolset, two additional clones from our RNA pool were chosen for biochemical analysis, based on their predicted structures[8]. One RNA, termed Clone 29, is unique for its potential formation of an almost-perfect terminator helix (Fig. 3.1a). The other RNA, termed Clone 10, was chosen for its lack of predicted structure and the potential for large conformational changes in the presence of ligand (Fig. 3.1b). Both clones contain mutations at nucleotide positions that evolved from the original RNA pool's expression platform, suggesting that these changes are important for function. Clone 29 is unique because this RNA only evolved from the ancestral SAM riboswitch at nucleotide positions 69, 88, and 97, thus almost identically matching the designed pool's expression platform, which was mutagenized at ~15 % per position in the antiterminator segment of the riboswitch. The conservation of this

segment in Clone 29, with respect to the original SAM riboswitch sequence thus has relatively low probability. For example a perfectly preserved (unmutated) ancestral sequence has a probability of occurrence of ~$(0.85)^N$, where N is the length of the segment mutated at 10 % level. For our starting pool, this segment was 29 nts long and the probability of ancestral sequence is thus ~$(0.85)^{29}$ = 0.009. The probability of isolating a sequence with three mutations in the segment is ~$(0.85)^{26}$ = 0.014. Clone 10 evolved at nucleotide positions: 69, 72, 86, and 91, thus also remaining similar to our starting pool. Clone 36 (the Were-1 photoriboswitch) also acquired mutations at position 72, but its other 8 mutations are where it differs from the ancestral SAM riboswitch and these do not overlap with Clone 10. Additionally, Clone 10 keeps the same terminator sequence from the starting pool except for two mutations at positions 86 and 91, indicating that it could possibly form a terminator when bound to amino-*t*SS or in ligand-free state.

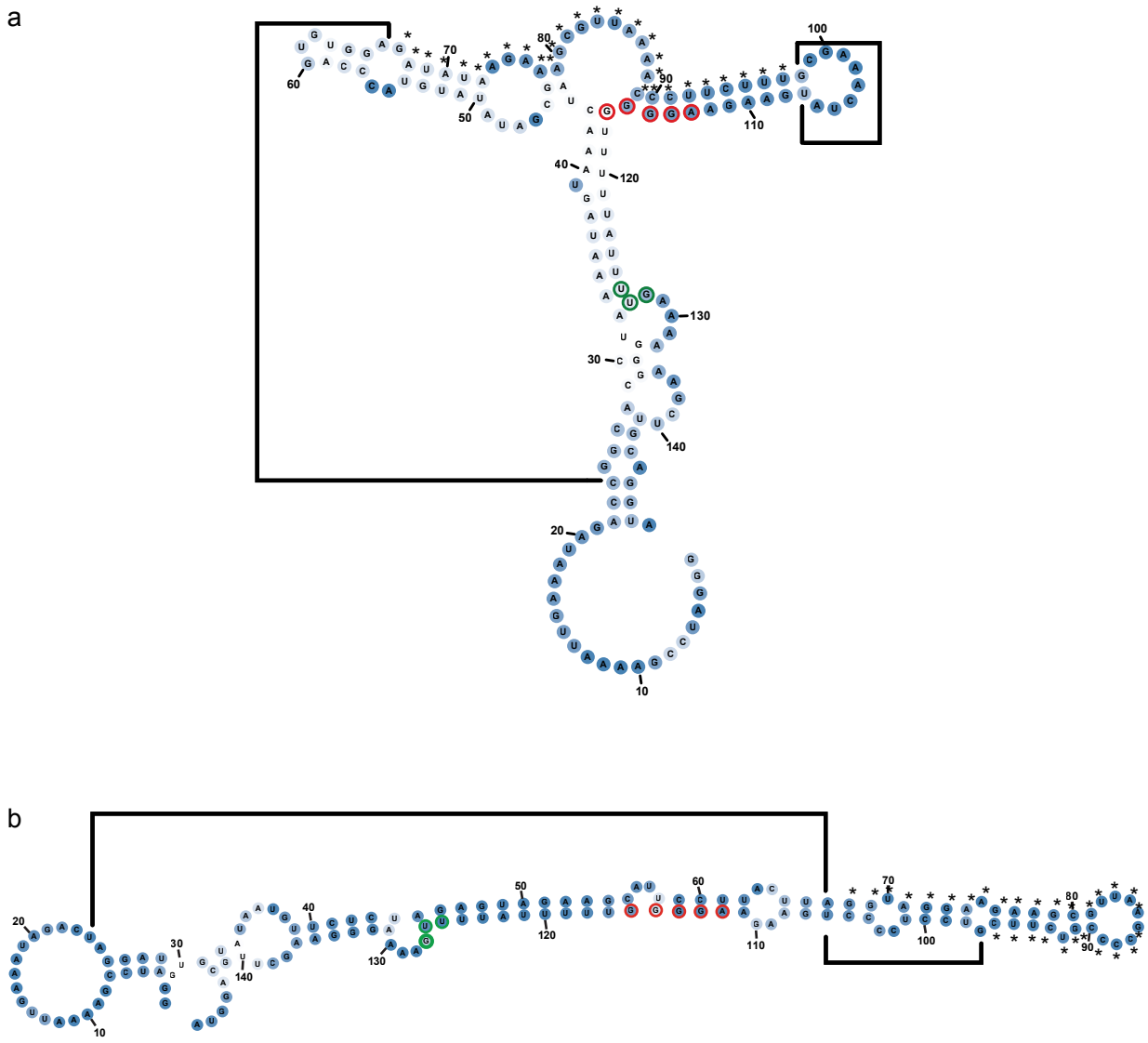

Figure 3.1. Predicted structures for Clone 29 and Clone 10. a, Secondary structure prediction of Clone 29 RNA in the absence of ligand. **b,** Secondary structure prediction of Clone 10 RNA in the absence of ligand. Both clones contain a Shine-Dalgarno sequence (red) and start codon (green) derived from the *B. subtilis mswA* SAM-I riboswitch. Base pair probability is demonstrated based on color intensity (blue).

Asterisks denote regions that were partially randomized in the starting pool. Brackets indicate regions that were fully randomized in the starting pool.

Because the terminator helix was mostly maintained, an *E. coli* promoter was added to the sequence in order to determine whether Clone 29 can regulate transcription termination, in future experiments, in the presence of amino-*t*SS. Using a toehold reporter that mimics ribosomal binding, toehold fluorescence was observed with increasing amino-*t*SS concentrations as Clone 29 was transcribed. In absence of ligand, toehold fluorescence slowly increased, suggesting that transcription was not completely terminated and the translation mimic was able to bind. However, upon adding in amino-*t*SS, toehold fluorescence increased, indicating that more RNAs folded into a conformation that allowed binding of the toehold and strand-displacement of the quencher DNA (Fig. 3.2a). Furthermore, when the same reaction was performed in the presence of three control ligands, the *cis* isoform of the stiff stilbene (amino-*c*SS), a commercial *trans* stilbene (tS) and a *trans* 4, 4 dihydroxystilbene (tDHS), there was no change in toehold fluorescence compared to the no-ligand control (Fig. 3.2b). The same experiments were performed for Clone 10 in parallel, for which a similar response was observed. In the presence of increasing amino-*t*SS concentrations, toehold fluorescence increased in comparison to the no-ligand control (Fig. 3.2c). Additionally, when control ligands (amino-*c*SS, tS, and tDHS) were added, there was no change in toehold fluorescence compared to the no-ligand control (Fig. 3.2d).

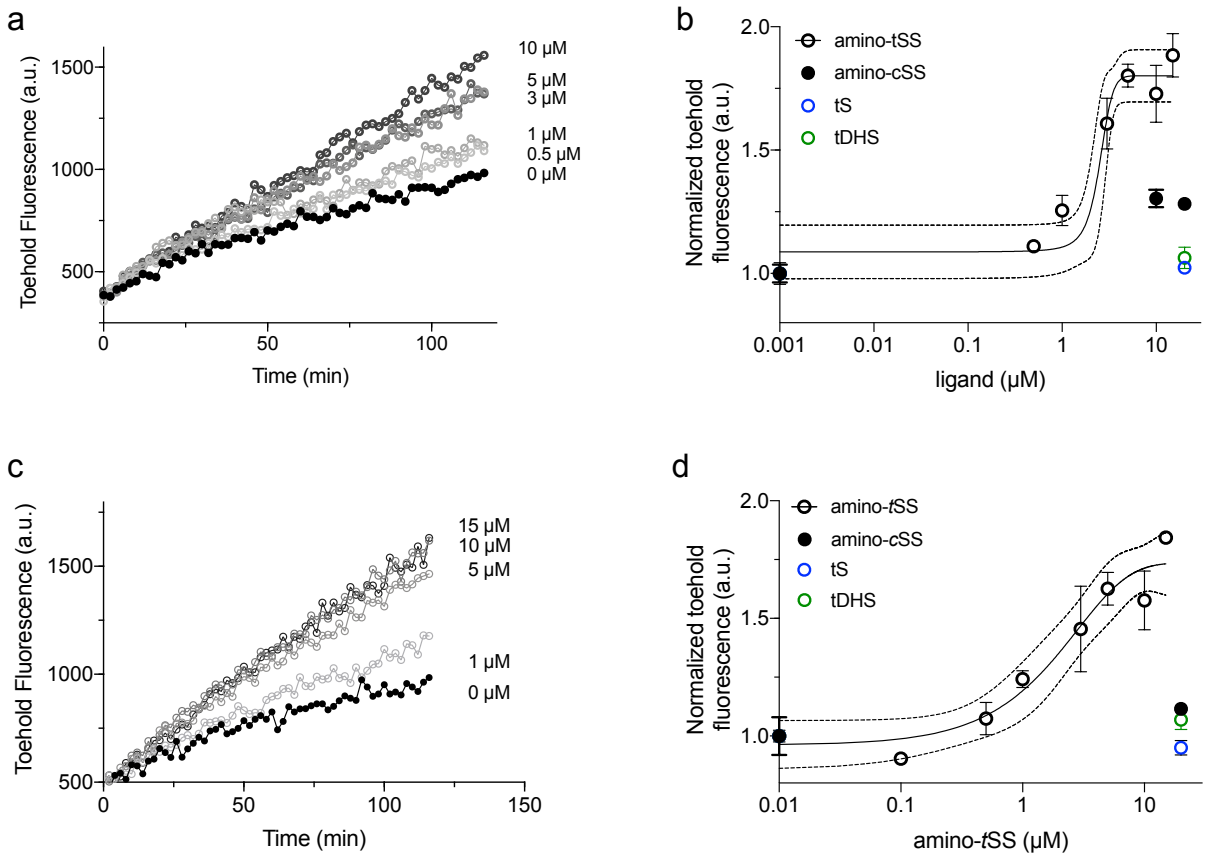

Figure 3.2 Co-transcriptional binding of a ribosome-mimic *in vitro*. a, Clone 29 binding to a ribosome-mimic in the presence of increasing amino-*t*SS using EcRNAP transcription. Toehold fluorescence increased with amino-*t*SS concentration, compared to the no-ligand control. **b,** Response (± SEM) of Clone 29 in the presence of amino-*t*SS and controls: amino-*c*SS (dark circles), tS (open, blue circle), and tDHS (open, green circle). Amino-*c*SS shows weak activation at higher concentrations. Dashed lines represent a 95% confidence interval. **c,** Clone 10 binding to a ribosome-mimic in the presence of increasing amino-*t*SS increased fluorescence over time compared to controls. **d,** Response (± SEM) of Clone 10 in the presence of amino-*t*SS, amino-*c*SS, tS, and tDHS. Dashed lines represent a 95% confidence interval.

To further study the kinetics of toehold binding of Clone 29 and Clone 10, a T7 promoter was added to their sequences in place of the *E. coli* promoter. The co-transcriptional toehold assay was repeated, now using Clone 29 in the presence of T7 RNAP, and an opposite response was observed. When no ligand was present, toehold fluorescence was robust, whereas in the presence of amino-*t*SS, toehold fluorescence decreased (Fig. 3.3a). Additionally, in the presence of amino-*c*SS, tS, and tDHS, there were no changes in toehold fluorescence compared to the no-ligand control (Fig. 3.3b). The same experiment was repeated for Clone 10, and a similar response was observed to that of Clone 29. In the presence of amino-*t*SS, toehold fluorescence decreased in a dose-dependent manner, whereas all control ligands (amino-*c*SS, tS, and tDHS) showed robust toehold fluorescence similar to the no-ligand control (Fig. 3.3c, d).

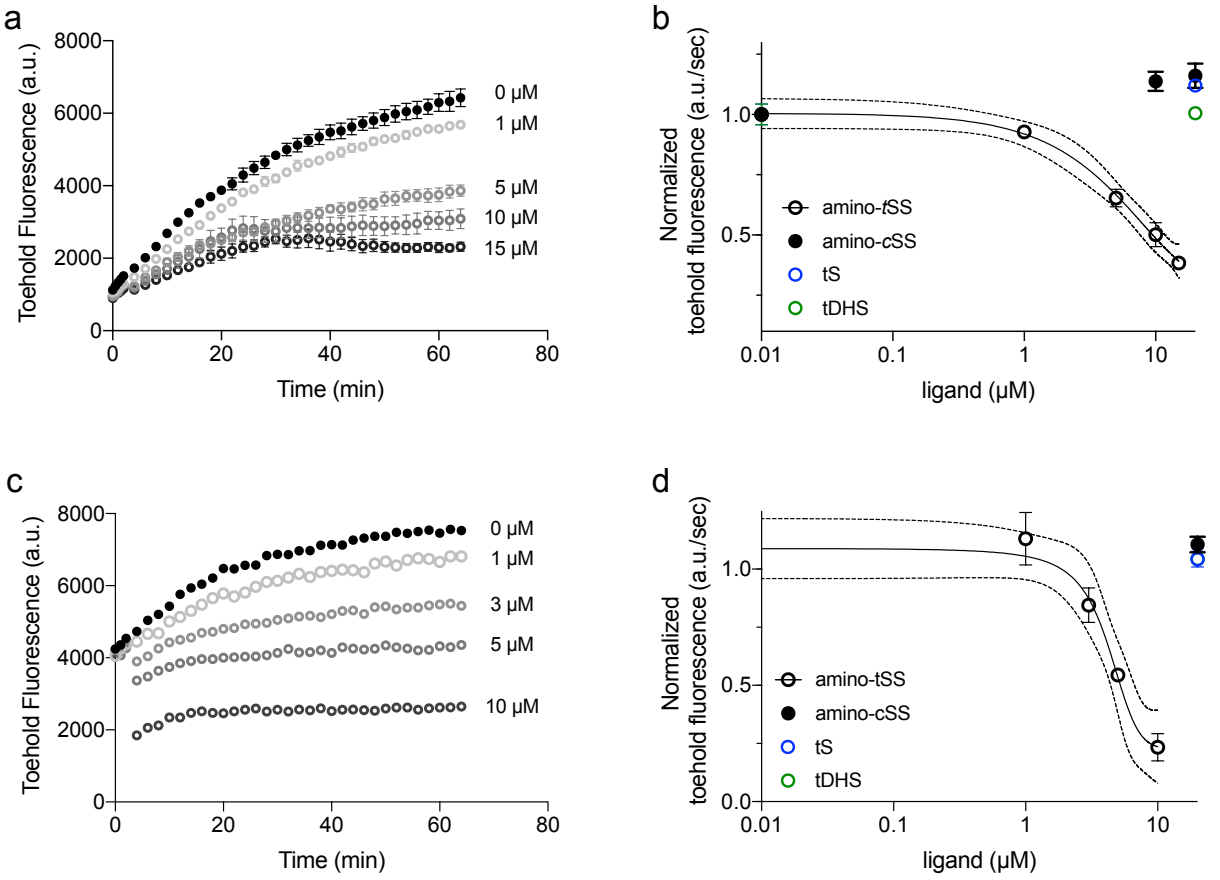

Figure 3.3 Co-transcriptional inhibition of a ribosome-mimic *in vitro*. a, Co-transcriptional response of Clone 29 to different concentrations of amino-*t*SS (μM) using the toehold reporter. Initial transcriptions of Clone 29 without ligand show identical increase in toehold fluorescence for all samples. When amino-*t*SS is added, a dose-dependent decrease in fluorescence is observed. **b,** Response (± SEM) of Clone 29 in the presence of amino-*t*SS, amino-*c*SS, tS, and tDHS. Dashed lines represent a 95% confidence interval. **c,** Co-transcriptional response of Clone 10 to different concentrations of amino-*t*SS (μM) using the toehold reporter. Similar to Clone 29, initial transcriptions of Clone 10 without ligand show identical increase in toehold fluorescence for all samples. After the addition of amino-*t*SS, fluorescence decreased in a dose-

dependent manner. **d,** Response (± SEM) of Clone 10 in the presence of amino-*t*SS, and controls: amino-*c*SS, tS, and tDHS. Dashed lines represent a 95% confidence interval.

3.3 Future Directions

Similar to SAM I, FMN, and adenine riboswitches, the *in vitro* folding of Clone 29 and Clone 10 appears to be transcription-rate limited[3,5,6]. To better understand the complexity of the system, more experiments need to be performed for Clone 29 and Clone 10. For example, both RNAs, with both sets of promoters, should be incorporated into a bacterial plasmid with a luciferase reporter to determine whether they can regulate translation *in vivo*. Additionally, both RNAs should be tested further *in vitro* to better understand whether they can act as co-transcriptional terminators. Co-transcriptional structural probing in the presence of various amino-*t*SS concentrations is also of interest.

To expand the toolset of optogenetic tools, it is important to test whether Clone 29 and Clone 10 are photoriboswitches. To classify each RNA as a photoriboswitch, these RNAs will have to regulate gene expression in response to light, co-transcriptionally or translationally, in a reversible manner. Based on the data we have gathered thus far, Clone 29 and Clone 10 have the potential to act as activators or inhibitors, depending upon the promoter–and by the extension speed of RNA synthesis–used to transcribe them. However, it is unclear in this current work whether both clones have high enough affinity for the *trans* isoform of our ligand over the *cis* isoform, as seen in Figure 3.2b. If Clone 29 is not specific enough for amino-*t*SS, then I hypothesize

that this RNA likely binds a similar component to both *trans* and *cis* stiff stilbene and this will likely impact its ability to be a photoriboswitch.

In conclusion, Clone 29 and Clone 10 are interesting RNAs that have maintained similar sequences to the ancestral riboswitch in the antiterminator region. Their structures suggest that they could form terminator helices to regulate transcription. Additionally, Clone 29 and Clone 10 show interesting kinetic responses to a ribosomal-mimic under different promoters. With an *E. coli* promoter, both RNAs activate strand displacement, mimicking translation activation *in vitro*. In contrast, with a T7 promoter, both RNAs inhibit strand displacement in the presence of amino-*t*SS, mimicking translational inhibition *in vitro*. Further analysis is needed to conclude if and how Clone 29 and Clone 10 regulate transcription and translation.

3.4 Materials and Methods

Reagents and equipment. Unless otherwise stated, all reagents were purchased from Sigma-Aldrich. (E)-6'-(2-aminoethoxy)-2,2',3,3' tetrahydro-[1,1'-biindenylidene]-6-ol (amino-*t*SS) was synthesized and prepared as previously described[8]. Commercially available reagents were used without further purification. Absorbance spectra were recorded with a Thermo Scientific NanoDrop 1000 spectrophotometer. Fluorescence excitation and emission spectra were measured with a BioTek Synergy H1 plate reader, unless otherwise specified.

***In vitro* RNA transcription**. RNA was transcribed at 37 ˚C for one hour in a 50 µL volume containing 40 mM tris-HCl, 6 mM dithiothreitol (DTT), 2 mM spermidine, 1.25 mM each rNTP, 8 mM $MgCl_2$, 1 unit of T7 RNA polymerase, and 5 pmol of DNA template. The transcripts were purified by 10 % PAGE under denaturing conditions (7 M urea). RNA was eluted from the gel into 300 µL of 300 mM KCl and precipitated by adding 700 µL of 95 % ethanol at –20 °C.

***In vitro* selection of amino-*t*SS aptamers.** An RNA pool derived from a *B. subtilis mswA* SAM-1 riboswitch, located in the 5′ untranslated region of the *metI* (cystathionine gamma-synthase, also denoted as *yjcI*) gene[9,10] was designed and RNAs were selected as previously described[8].

Screening of potential amino-*t*SS binders. *Clone 29.* Following the sixth round of *in vitro* selection, RNAs were tested for their binding activity to amino-*t*SS based on their

optical properties. Clone 29 showed the second highest (after Were-1) increase in amino-*t*SS fluorescence at 410 nm and was chosen for further analysis.

Clone 10. After six rounds of *in vitro* selection, the selected pool was cloned into a pBV-Fluc plasmid (addgene) and transformed into DH5α *E. coli* cells. Cells were plated on agar containing carbenicillin and incubated overnight at 37 ˚C. Individual colonies were picked from the master plate and inoculated overnight in Luria Broth containing Carbenicillin. Plasmids were extracted and purified using a Miniprep Kit (QIAGEN), and sequenced (GENEWIZ). One clone, Clone 10, was chosen for further analysis based on its predicted secondary structure.

***In vitro* co–transcriptional toehold-binding kinetics of Clone 29 and Clone 10**. An *E. coli* promoter was added in front of each clone's DNA sequence using PCR (Supplementary Table 3.1). *In vitro* transcription was performed similarly to the above–described RNA transcription assay with the following modifications: 10 mM $MgCl_2$, 18 nM template DNA, 0.01% Triton X- 100 pH 7.5 @ 25°C, 1 unit of *E. coli* RNA polymerase and 50 nM toehold-fluorophore reporter were used, without spermidine. A 30 μL transcription reaction was initiated by the addition of 8 mM rNTP mix (containing 2 mM of each rNTP) and fluorescence emission of the toehold-fluorophore reporter was recorded under continuous illumination at 37 °C using the following parameters: excitation wavelength, 485 nm; emission wavelength, 520 nm; increment of data point collection, 2 mins. These conditions were used for the entire experiment, unless stated otherwise. After an initial fluorescence increase, corresponding to the initial burst of

transcription, amino-*t*SS was rapidly added to the solution and fluorescence emission was recorded for up to three hours. Controls, amino-*c*SS, tS, and tDHS, were examined alongside amino-*t*SS reactions to ensure specificity for the target ligand.

A T7 promoter was incorporated in front of Clone 29 and Clone 10 DNA sequences using PCR, replacing the location of the *E. coli* promoter. *In vitro* transcription was performed similarly to the T7 polymerase transcription (above) with the following modifications to mimic $MgCl_2$ concentrations in the *E. coli* polymerase experiments: 6 mM $MgCl_2$, 3 pmol template DNA and 50 nM toehold-fluorophore reporter were used. A 30 µL transcription reaction was initiated by the addition of 4 mM rNTP mix (containing 1mM of each rNTP) and fluorescence emission of the toehold-fluorophore reporter was recorded under continuous illumination at 37 °C following the same parameters described above. Controls, amino-*c*SS, tS, and tDHS, were examined alongside amino-*t*SS reactions to ensure specificity for the target ligand.

Supplementary Table 3.1 | DNA sequences used for *in vitro* analysis of Clone 29 and Clone 10.

E. coli promoter C29	Gaattctttacactttatgcttccggctcgtatgttgtgtggaattgtgagcggat aacaattGGGATCCGAAAATTGAAATAGACCGGCACCT AAAATAGTAAACTCGATATATGTACCCAGTGTGGAG ATATAAGAAGAAGCGTTAAAACCCTTCTTTGCGAAA CTATGAAGAAGGGGTTTTTATTTTGAAAAGGGAAGCTTGCAGG
E. coli promoter C10	Gaattctttacactttatgcttccggctcgtatgttgtgtggaattgtgagcggat aacaattGGGATCCGAAAATTGAAATAGACTAGGATTG TATAATGTTCTCTAGAGTAGAAGCATTCCTTACTTAG GTAGGAAGAAGCGTTAAGCCCCGTCTTCGTCCTCCC CTGAAGAAGGGGTTTTTATTTTGAAAAGGGAAGCTTGCAGG
T7 promoter C29	TAATACGACTCACTATAGGGATCCGAAAATTGAAATA GACCGGCACCTAAAATAGTAAACTCGATATATGTACC CAGTGTGGAGATATAAGAAGAAGCGTTAAAACCCTTC TTTGCGAAACTATGAAGAAGGGGTTTTTATTTTGAAAA GGGAAGCTTGCAGG
T7 promoter C10	TAATACGACTCACTATAGGGATCCGAAAATTGAAATA GACTAGGATTGTATAATGTTCTCTAGAGTAGAAGCAT TCCTTACTTAGGTAGGAAGAAGCGTTAAGCCCCGTC TTCGTCCTCCCCTGAAGAAGGGGTTTTTATTTTGAAA AGGGAAGCTTGCAGG

3.5 References

1. Uhm, H., Kang, W., Ha, K. S., Kang, C. & Hohng, S. Single-molecule FRET studies on the cotranscriptional folding of a thiamine pyrophosphate riboswitch. *Proc. Natl. Acad. Sci. U. S. A.* **115,** 331–336 (2017).
2. Watters, K. E., Strobel, E. J., Yu, A. M., Lis, J. T. & Lucks, J. B. Cotranscriptional Folding of a Riboswitch at Nucleotide Resolution. *Nat. Struct. Mol. Biol.* **23,** 1124 (2016).
3. Lutz, B., Faber, M., Verma, A., Klumpp, S. & Schug, A. Differences between cotranscriptional and free riboswitch folding. *Nucleic Acids Res.* **42,** 2687–2696 (2014).
4. Winkler, W. C. & Breaker, R. R. Genetic control by metabolite-binding riboswitches. *ChemBioChem* **4,** 1024–1032 (2003).
5. Wickiser, J. K., Winkler, W. C., Breaker, R. R. & Crothers, D. M. The speed of RNA transcription and metabolite binding kinetics operate an FMN riboswitch. *Mol. Cell* **18,** 49–60 (2005).
6. Lemay, J. F. *et al.* Comparative study between transcriptionally- and translationally-acting adenine riboswitches reveals key differences in riboswitch regulatory mechanisms. *PLoS Genet.* **7,** (2011).
7. Rieder, R., Lang, K., Graber, D. & Micura, R. Ligand-induced folding of the adenosine deaminase A-riboswitch and implications on riboswitch translational control. *ChemBioChem* **8,** 896–902 (2007).
8. Rotstan, K. A. *et al.* Regulation of mRNA translation by a photoriboswitch. *bioRxiv* 761775 (2019). doi:10.1101/761775

9. Grundy, F. J. & Henkin, T. M. The S box regulon: a new global transcription termination control system for methionine and cysteine biosynthesis genes in gram-positive bacteria. *Mol. Microbiol.* **30,** 737–49 (1998).

10. Winkler, W. C., Nahvi, A., Sudarsan, N., Barrick, J. E. & Breaker, R. R. An mRNA structure that controls gene expression by binding S-adenosylmethionine. *Nat. Struct. Biol.* **10,** 701–707 (2003).